Single-Cell Profiling Reveals Altered Endometrial Cellular Features Across the Menstrual Cycle in Endometriosis Patients

Ana Almonte-Loya[1,2,3], Wanxin Wang[4], Sahar Houshdaran[4], Xinyu Tang[1], Emily Flynn[2], Binya Liu[4], Divyashree Kushnoor[2], Camran Nezhat[5], Felipe Vilella[6,7], Carlos Simon[6,7,8,9], Kim Chi Vo[4], Amber Casillas[4], Umair Khan [1,3], Carlota Peredas[1,10], Tomiko T. Oskotsky[1,11], David Huang[4], Júlia Vallvé-Juanico[4], Juan Irwin[4], Alexis Combes[2]*, Marina Sirota[1]*, Gabriela Fragiadakis[2]*, Linda Giudice[4]*

Affiliations:

1. Bakar Computational Health Sciences Institute, University of California, San Francisco
2. CoLabs, University of California San Francisco, San Francisco, CA, USA
3. Biological and Medical Informatics Program, University of California San Francisco, San Francisco, USA
4. Center for Reproductive Sciences, Department of Obstetrics, Gynecology and Reproductive Sciences, University of California, San Francisco, San Francisco, CA
5. Camran Nezhat Institute, Center for Special Minimally Invasive and Robotic Surgery, Woodside, CA 94061, USA
6. Carlos Simon Foundation, Valencia, Spain
7. INCLIVA Biomedical Research Institute, Valencia, Spain
8. Department of Pediatrics, Obstetrics and Gynecology, School of Medicine, University of Valencia, Valencia, Spain

9. Department of Obstetrics and Gynecology, Beth Israel Deaconess Medical Center, Harvard Medical School, Boston, MA, USA
10. Pharmaceutical Sciences and Pharmacogenomics Program, University of California San Francisco, San Francisco, USA
11. Division of Clinical Informatics and Digital Transformation, Department of Medicine, University of California San Francisco, San Francisco, CA, USA

Abstract

Endometriosis is a chronic, estrogen-dependent condition affecting over 190 million women globally, characterized by the ectopic presence of endometrial-like tissue that leads to inflammation, pain, and infertility. Despite its prevalence, the pathogenesis of endometriosis remains poorly understood. Here, we present a comprehensive single-cell transcriptomic atlas comprising 228,000 cells derived from 43 eutopic endometrial biopsies from patients with endometriosis, fibroid controls and healthy controls, sampled across the menstrual cycle. This analysis reveals previously uncharacterized subpopulations of endometrial fibroblasts and epithelial cells undergoing epithelial–mesenchymal transition, alongside disrupted immune cell communication networks. Comparative gene expression profiling implicates oxidative stress, aberrant cell migration, and dysregulated apoptosis as central features of the disease state. These findings suggest that endometriosis alters eutopic endometrial homeostasis, with potential consequences for fertility, regeneration, and disease progression. Our dataset provides a valuable resource for biomarker discovery and identifies candidate therapeutic targets aimed at restoring endometrial function and alleviating symptoms in affected individuals.

Introduction

Endometriosis is a common, estrogen-dependent inflammatory disease characterized by the ectopic growth of endometrial-like tissue outside the uterus. Most disease resides in the pelvia and is associated with inflammation, chronic pelvic pain, pain with intercourse and menses, and and infertility[1–5]. It affects around 10% of reproductive-age individuals with a uterus[2–4], equating to approximately 190 million cases worldwide[2,6]. The economic burden in the U.S. alone exceeds $22 billion[7,8]. Despite decades of research and some advancements in exploring the disease's pathobiology, effective individualized management remains challenging, primarily because of the heterogeneous nature of endometriosis phenotypes and symptoms, and involvement of systemic components[2,4].

Although retrograde menstruation is a widely proposed origin of endometriosis, bone marrow stem cells may also contribute to its pathogenesis, and understanding eutopic (within the uterus) endometrial alterations in patients with disease remains limited, particularly in relation to tissue dyshomeostasis throughout the menstrual cycle and impact on fertility and pregnancy outcomes[1–4,9]. Since the endogenous ovarian steroids, estradiol and progesterone, are key regulators of endometrial gene expression[9–11], investigating endometrial features across the menstrual cycle is key to understanding how aberrancies of signaling by these hormones drive endometrial dysfunction in endometriosis patients[4,9].

Single-cell analysis has emerged as a powerful tool to decipher the complexities of diseases like endometriosis, offering detailed insights into the cellular heterogeneity of the eutopic and ectopic endometrium[9,12–17]. Recent studies utilizing these advanced methodologies have revealed diverse roles of immune cells, stromal fibroblasts, and epithelial cells in the eutopic endometrium proper and in relation to tissue dysfunction and pathogenesis and pathophysiology of endometriosis lesions. These studies have shown that eutopic endometrium in endometriosis patients exhibits epithelial abnormalities and dysregulated signaling pathways affecting tissue

homeostasis. Moreover, analysis of menstrual endometrium, a "liquid biopsy" of late secretory phase endometrium, reveals aberrant progesterone signaling in stromal fibroblasts, which are essential for pregnancy establishment and success and endometrial regeneration[9,13]. These findings underscore the importance of cellular diversity and functional interactions in the eutopic endometrium of patients with endometriosis and highlight potential avenues for targeted therapeutic interventions.

In this study, we utilized single-cell RNA sequencing (scRNA-seq) to examine cellular and molecular changes as well as cell-cell communication patterns in the eutopic endometrium of patients with and without endometriosis across disease severities and menstrual cycle phases. By profiling the eutopic endometrium, we aimed to identify cycle phase-dependent alterations in key cell populations, including stromal fibroblasts, unciliated epithelial cells, EMT cells, and immune dysregulation in macrophages and uterine natural killer (uNK) cell types and subtypes. Through these analyses, we sought to map critical cell-cell signaling pathways involved in inflammation, apoptosis, and migration, offering deeper insights into the molecular mechanisms driving endometrial dysfunction in patients with endometriosis.

Results

Diverse cellular cartography of the eutopic endometrium

By using multiplexed single-cell RNA sequencing to mitigate batch effect and other technical artifacts, single-cell analyses identified 228,021 cells from the eutopic endometrium of 43 participants, including 25 with endometriosis, 8 with no known reproductive disorders (“pristine” controls), and 10 with uterine fibroids and no endometriosis (“fibroid” controls). Patient

94 samples were stratified according to case/control, menstrual cycle phase and endometriosis
95 severity[18] (**Fig. 1A, Supplementary Table 1**). Following experimental processing, samples
96 were processed in silico including quality filtering, integration, and batch correction, prior to
97 downstream computational analysis (**Fig. 1B, Methods**).
98 Using established cell markers and visualizing using Uniform Manifold Approximation
99 and Projection (UMAP) visualization, we identified thirty-two clusters representing six major cell
100 types: immune cells, stromal fibroblasts, ciliated epithelial cells, unciliated epithelial cells,
101 endothelial cells, and vascular smooth muscle cells (VSM) (**Fig. 2A, SFig. 1A, STable 2**). We
102 then explored the distribution of menstrual phases and disease states within these cell clusters.
103 Coloring the UMAP based on these characteristics showed distinct regions for proliferative and
104 secretory phases (**Fig. 2B and SFig. 1B**), as well as separations between endometriosis, fibroid
105 control, and pristine control (**Fig. 2C and SFig. 1C**). Menstrual phase, disease status, and
106 libraries were distributed across all cell types (**SFig. 1D-G**). Principal component analysis (PCA)
107 of the cell composition profile per sample further confirmed changes in endometrial cellular
108 composition driven by menstrual cycle phase and disease condition (**Fig. 2D,E**). Notably, the
109 separation among conditions (endometriosis, fibroid controls, and pristine controls) was less
110 pronounced than differences driven by cycle phase. Similar to the cellular composition analysis
111 results, most cell types showed significant transcriptional differences between proliferative and
112 secretory phases in fibroblast and unciliated epithelia populations (**SFig. 2-4, Supplementary**
113 **Note, STable4)**. Interestingly, although endometrium from patients affected by fibroids exhibited
114 distinct signals, their molecular signatures were more similar to endometriosis than to pristine
115 controls in certain cell types (examples in **SFig.5, Supplementary Note** below, **STable5**). Thus,
116 we focused downstream analyses on comparing eutopic endometrium signatures in
117 endometriosis and pristine controls, stratified by menstrual cycle phase (**Fig. 2F**).
118

Differential gene expression across cell types in endometrial pathology

We first examined differentially expressed genes (DEGs) filtering by adj. p-val < 0.05 and |log2FC| > 0.25, between endometriosis and pristine controls in the five non-immune broad cell types (**STable 3**) (**SFig. 6**). In both the proliferative and secretory phrases, we saw the highest numbers of DEGs in stromal fibroblasts (n=338 and n=1384 respectively) followed by unciliated epithelial cells (n=482 and n=983) and endothelial cells (n=58, n=417). VSM and ciliated epithelial cells also showed DEGs, mainly in the secretory phase (n=5 and n=88 for VSM, n=4 and n=84 for CE) (**SFig. 6**).

We found that all non-immune cell types had more DEGs in the secretory phase than in the proliferative phase (**Fig. 2G, H**). Although most gene differences generally appeared to be phase-specific (**SFig. 7A-E.**), there was greater overlap of DEGs across cell types in the secretory phase compared to the proliferative phase (**Fig. 2G, H**).

These findings suggest that endometriosis exerts greater transcriptional effects in secretory phase endometrium, which may have significant implications for fertility and reproductive health. To investigate if the observed DEGs are isolated to specific endometriosis severity groups, we also performed similar comparisons stratified by endometriosis stage, which showed general concordance with the transcriptomic differences seen in the analyses without endometriosis severity stratification (**SFig8, Supplementary Notes, STable6,7**). Therefore, we continued with an analysis approach unstratified by endometriosis stage.

Distinct biological process alterations between menstrual cycle phases in stromal fibroblasts in endometriosis cases

We decided to investigate the two main mesenchymal-derived cell populations, stromal fibroblast and VSM (**Fig. 3A**). Given the large number of significant DEGs in stromal fibroblasts in endometriosis compared to pristine controls, we first focused the on the signatures of this cell population. We found 204 overlapping DEGs between the proliferative phase and secretory phase, among which 156 genes consistently exhibited either upregulation or downregulation in both phases in patients with endometriosis compared to pristine controls (**Fig. 3B, SFig. 9A**). The top upregulated DEGs included genes related to heat shock proteins (HSPs), specifically isoforms of *HSP70* - known to protect cellular damage caused by stress and inflammation,[19,20] as well as for their functions as steroid hormone receptor chaperones, cell cycle regulators, and regulators of apoptosis[21]. These include *HSPA6* (adj. p-val <0.001, log2FC = 0.77 vs 2.88 for proliferative and secretory phases, respectively) and *CRYAB* (adj. p-val <0.001, log2FC = 1.36 for proliferative; adj. p-val < 0.001, log2FC = 2.48 for secretory phase). The top downregulated genes included *SFRP4* (adj. p-val< 0.001, log2FC = -1.04 for proliferative and adj. p-val<0.001, log2FC = -1.54 for secretory phase) and *SFRP1* (adj. p-val<0.001, log2FC = -0.44 for proliferative, adj. p-val<0.001, log2FC = -1.04 for secretory phase) that encode these frizzle related proteins (SFRP4, SFRP1), inhibitors of Wnt signaling[22]. The remaining 48 overlapping DEGs exhibited phase-dependent expression patterns with opposing alteration directions between the proliferative and secretory phases (**SFig. 9A**).

We applied Gene Set Enrichment Analysis (GSEA) to understand the pathway changes implicated in endometriosis versus pristine controls in the proliferative and secretory phases independently (**Fig. 3C, STable 14**). Our results showed that in the secretory phase, pathways related to heat response and protein folding were upregulated, which could represent reactive

164 oxygen species (ROS) accumulation in this phase in disease versus control. Other apoptotic
165 and programmed cell death pathways were additionally identified in endometriosis, as well as
166 enrichment related to response to metal ion (**STable 14**).
167

168 Endometrial stromal fibroblast subpopulations associated with 169 endometriosis

170 To further explore these phase-specific disease phenotypes in more detail, we sub-
171 clustered stromal fibroblasts and VSM populations and annotated them based on canonical
172 markers, which resulted in eight subpopulations (**Fig. 3D-E, STable 2, Methods**). Among the
173 identified fibroblast clusters, we found activated fibroblast cells, a proliferating cluster, and a
174 previously described SFRP4+ population in endometrial fibroblasts[23]. Additionally, other distinct
175 stromal fibroblast clusters were identified, with IGF1+, MMP+, HSP+, and WFDC2+ markers.
176 Each subpopulation had different distributions related to the menstrual phase and disease
177 status (**SFig. 9B-D**). All subpopulations were observed across all libraries (**SFig. 9E-F**).
178 We compared cell type composition between endometriosis and pristine controls,
179 stratifying samples between secretory and proliferative menstrual phases (**SFig. 9G**). During the
180 proliferative phase, the SFRP4+ subpopulation was less abundant in endometriosis patients (p-
181 adj. < 0.009) (**Fig. 3F**). This cell population has been described to be abundant during the
182 endometrium's regenerative phase[23,24].In the secretory phase, the fraction of HSP+ stromal
183 subpopulation was significantly higher in cases versus controls (p-adj. < 0.0001) (**Fig. 3F**). This
184 HSP+ population has not been previously observed in endometrial fibroblast tissue. However, it
185 has been described in other fibroblast tissues under stress conditions[25]. Their role may be
186 significant in collagen production and fibrosis processes[26,27].

187 Furthermore, the differences between secretory and proliferative proportions were
188 significant in activated fibroblasts (p-adj. < 0.05). Activated fibroblasts drive wound healing and
189 are linked to cancer through their contractile, ECM-producing, and inflammatory roles[28]. The
190 same difference in proportion was observed in the HSP+ population (p-adj. < 0.01) in cases
191 (**SFig. 9H**).

192 At the transcriptional level, phase-specific differential expression was observed in
193 several subpopulations when comparing cases to pristine controls (**Fig. 3G, STable 8,9, SFig.**
194 **10-11)**. We investigated the activated fibroblast population, which during the proliferative phase
195 exhibited the most differences compared to pristine controls (adj. p-val < 0.05 and |log2FC|>
196 0.25, n=100 DEG) (**Fig. 3G**). The top upregulated genes include *TANGL* (adj. p-val < 0.01,
197 log2FC = 1.87) and *CAV1* (adj. p-val < 0.001, log2FC = 1.26), both biomarkers of cancer-
198 associated fibroblasts[28–30]. *NFKBIA* (adj. p-val < 0.001, log2FC = 1.25), a regulator of the
199 inflammatory response, and *KLF6* (adj. p-val < 0.001, log2FC = 1.05), which regulates
200 proliferation and apoptosis of endometrial stromal cells[31], were also significantly upregulated.

201 Conversely, the downregulated genes included *IGFBP5* (adj. p-val < 0.001, log2FC = -
202 1.92), implicated in early responses during the development of fibrosis[32], and *PENK* (adj. p-val <
203 0.05, log2FC = -1.74), associated with the induction of apoptosis[33] (**Fig. 3H**).

204 The HSP+ population, also included differences in transcriptomic signature
205 endometriosis compared to controls, specifically during the proliferative phase (adj. p-val < 0.05
206 and |log2FC| > 0.25, n=48 DEG) (**Fig. 3G,H**). Downregulated genes included *IGFBP5* (adj. p-val
207 <0.001, log2FC=-1.66) and *SFRP4* (adj. p-val <0.001, log2FC=-1.66). Conversely, upregulated
208 genes included *GADD45B* (adj. p-val <0.01, log2FC=1.05), which relates to stress response
209 and immune regulation[34], *TCIM* (adj. p-val <0.001, log2FC=0.67), a positive regulator of the
210 Wnt/beta-catenin signaling pathway[35], as well as *KLF6* (adj. p-val <0.001, log2FC=0.56) and
211 *NFKBIA* (adj. p-val <0.001, log2FC=0.68), which were also observed in activated fibroblasts.

212 Other important upregulated genes that play a role in immune response[36] were *FOS* (adj. p-val
213 <0.001, log2FC=0.63) and *JUN/JUNB* (adj. p-val <0.001, log2FC=0.56 and log2FC=0.56,
214 respectively) (**Fig. 3H**). GSEA revealed that this HSP+ subpopulation exhibited an increase in
215 immune response development and cellular response to stress (adj. p-val < 0.05) (**Fig. 3I**).

216 Proliferating fibroblasts also exhibited notable differences during the proliferative phase
217 in cases compared to controls. This subpopulation showed upregulation of genes including
218 *CCN2* (adj. p-val<0.001, log2FC= 0.76) (**SFig. 11F**), which plays a critical role in cell
219 proliferation, differentiation, and adhesion.

220 We next aimed to investigate the VSM cells. This population clustered closely with the
221 stromal fibroblast population, perhaps due to their shared mesenchymal lineage and other
222 biological similarities. For instance, VSM cells can convert into myofibroblasts during wound
223 healing and fibrosis, and vice versa, stromal fibroblasts are also able to transform into
224 myofibroblasts in inflammatory environments[37]. In addition to VSM, we also examined WFDC2+
225 fibroblasts that express WFDC2, a marker in cancer-associated fibroblasts[38]; additionally, this
226 gene has been shown to promote fibroblast-myofibroblast transition in pulmonary cells[39,40].
227 Given this similarity, we hypothesize both cell types may play shared roles in the development
228 of endometriotic lesions.

229 In the secretory phase, VSM exhibited the highest number of DEGs in cases compared
230 to pristine controls (adj. p-val < 0.05 and |log2FC| > 0.25, n=122 DEG). (**Fig. 3G**). WFDC2+
231 fibroblasts (WFDC2+ F) also exhibited a significant number of DEGs (n=49 DEG) (**Fig. 3G**).

232 Both subpopulations had upregulated DEGs involving heat shock-related proteins that
233 protect cells from stress-induced damage. These included *HSPA6* (adj. p-val <0.001, log2FC =
234 2.23 in VSM) (adj. p-val <0.001, log2FC = 3.85 in WFDC2+ F), *HSPA1B*, (adj. p-val <0.001,
235 log2FC = 1.93 in VSM) (adj. p-val <0.001 log2FC =2.99 in WFDC2+ F) and *CRYAB* (adj. p-val
236 <0.001, log2FC = 1.43 in VSM) (adj. p-val <0.001, log2FC = 2.46 in WFDC2+ F.) (**Fig. 3H**).

237 Downregulated genes in both subpopulations included *SFRP1* (adj. p-val <0.001, log2FC = -
238 0.80 in WFDC2+ F), (adj. p-val <0.001, log2FC = -0.41 in VSM.), whose suppression may
239 promote cell proliferation and migration[41] (**Fig. 3H**). Consistently, GSEA showed the
240 upregulation of heat-stimulated pathways in both subpopulations and a common response to
241 stress. Additionally, as a result of this heat shock protein-related signature, VSM showed
242 enrichment of distinct patterns of regulation of apoptosis, including negative regulation of cell
243 death and programmed cell death, as well as immune response, showing regulation of cytokine
244 production (**Fig. 3I, STable 14**).

245 Increased motility and migration in unciliated epithelial cells during the 246 secretory phase

247 Since unciliated epithelial cells consistently exhibited high transcriptional changes in
248 cases, we compared their expression patterns stratified by proliferative and secretory phases
249 (**Fig. 4A, B, STable 3**). Genes that were consistently upregulated throughout the menstrual
250 cycle in cases included those related to immunomodulation, e.g. *PAEP* (*progesterone-*
251 *associated endometrial protein*) (adj. p-val <0.001, log2FC = 2.59 and adj. p-val <0.001, log2FC
252 = 2.29 in proliferative and secretory phases, respectively) and i*nterferon stimulated gene 15*
253 (*ISG15*) (adj. p-val <0.001, log2FC = 0.31 and adj. p-val <0.001, log2FC = 0.78 in proliferative
254 and secretory phases, respectively), (**Fig. 4B, SFig. 12A**). In contrast, *SOX4*, a potential
255 negative modulator for cell proliferation[42], was downregulated in cases in both phases (adj. p-val
256 <0.001, log2FC = -0.32 in proliferative, adj. p-val <0.001, log2FC =-1.4 in secretory phase)
257 (**Fig. 4B**). Significant upregulation of pathways related to cell motility and migration were noted
258 in the secretory phase (**Fig 4C**), as well as an increased response to metal ion, similar to
259 fibroblast cells (**STable 14**). This prompted further investigation into the specific epithelial
260 subpopulations driving these changes.

261

262 ## Endometrial glandular epithelial cells expressed genes associated

263 with endometriosis and pregnancy

264 Eight distinct epithelial cell subpopulations were identified using canonical and reported
265 markers (**Fig. 4D,E, STable 2, Methods**). These comprised four glandular epithelial
266 populations, two epithelial-to-mesenchymal transition cells (EMT) subpopulations (one *VIM*+
267 and one with collagen-related gene expression), a progenitor cell population (*MUC5B*+ and
268 *TFF3*+)[14], and a large ciliated epithelial cell (CE) subpopulation previously mentioned.
269 We observed pronounced variations in subpopulation composition across menstrual
270 cycle phases (**SFig. 12B**) and disease condition (**SFig. 12C,D**). Some subpopulations, here
271 labeled glandular E3 and glandular E4, were composed of specific libraries or samples (**SFig.
272 12E-F**). Exploring differences in cell type proportion per sample showed no significant changes
273 between endometriosis and controls (**SFig. 12G,H**).
274 In the proliferative phase, several epithelial subpopulations exhibited notable
275 transcriptional differences between cases and controls (**Fig. 4F, STable 10-11, SFig. 13 ,14).** In
276 glandular E1, we identified 870 DEGs between endometriosis and pristine controls during the
277 proliferative phase. Genes upregulated in this subgroup were also upregulated in the larger
278 category of unciliated epithelial cells, including expression of *PAEP* (adj. p-val <0.001,
279 log2FC=4.06) (**Fig. 4G**). GSEA using glandular epithelium DEGs revealed distinct pathway
280 alterations associated with endometriosis. In particular, pathways associated with “Female
281 pregnancy” and “Response to steroid hormones” were enriched (**Fig. 4H**), and several genes
282 belonging to these pathways were upregulated in endometriosis cases, including *SPP1, MMP7,*
283 *IGFBP7, FOSB, LIF,* and *SLC2A1* (**STable 10,14**). While these genes are crucial for pregnancy
284 and fertility, they are also implicated in the pathophysiology of endometriosis[43–48]. Additionally,

285 a gene related to immune response in the endometrium[49], *CD74*, was upregulated (adj. p-val
286 <0.001, log2FC=1.09) (**STable 10**). These findings highlight the complex endometrial
287 microenvironment in the setting of endometriosis
288

289 EMT epithelial subtypes dominate the changes in unciliated epithelial 290 cells

291 During the secretory phase, two main subpopulations exhibited differences at the
292 transcriptional level between endometriosis patients and pristine controls: EMT1 and CE cells
293 (adj. p-val < 0.05 and |log2FC| >0.25, n=533 DEG for EMT1 and n=75 for CE) (**Fig. 4F**). In
294 particular, *CRYAB* (adj. p-val <0.001, log2FC=1.82 for EMT1, log2FC=2.01 for CE) was
295 differentially expressed in both subpopulations (**Fig. 4G**). This upregulation seen in EMT1 and
296 CE cells is also common to other cell types, such as fibroblasts and VSM. Uniquely, EMT1
297 showed upregulation of pathways related to cell migration, locomotion, motility, and adhesion
298 (**Fig. 4H**). The genes driving this enrichment were *CCL20*, (adj. p-val <0.001, log2FC=2.20),
299 *CXCL14* (adj. p-val <0.001, log2FC=1.95), *IGFBP7* (adj. p-val <0.001, log2FC=0.68), and
300 *GADD45A* (adj. p-val <0.001, log2FC=0.98). Furthermore, we observed a decrease in the
301 regulatory processes of the canonical Wnt signaling pathway (**STable 14**) with inhibitors *SFRP1*
302 and *SFRP4* downregulated, suggesting activation of the WNT beta-catenin pathway. In contrast,
303 CE showed an upregulation of pathways related to apoptosis and cell death (**Fig. 4H**). These
304 data underscore unique phase-specific differences in epithelial subtype gene expression in
305 endometrium from endometriosis patients.
306

Endothelial cells show leukocyte migration and inflammation associated with endometriosis

Endothelial cells exhibited a significant number of DEGs in cases versus controls across menstrual cycle phases (**STable 3**). Notably, genes involved in vascular function and inflammation, such as *KLF6* (adj. p-val <0.001, log2FC=1.77 in secretory phase; adj. p-val <0.01, log2FC=0.61 in proliferative phase), *ICAM1* (adj. p-val <0.001, log2FC=1.79 in secretory phase), and *APOLD1* (adj. p-val <0.001, log2FC=0.62 in secretory phase), were upregulated in endometriosis cases (**SFig. 6G,H**). GSEA again revealed upregulated pathways related to heat shock protein response and oxidative stress in the secretory phase, emphasizing the impact of endometriosis on these key biological processes across cell types. Moreover, enrichment of leukocyte migration was noteworthy in the secretory phase, alongside regulation of cytokine expression in both menstrual phases (**SFig. 7F, STable 14**), thus highlighting the interaction between endothelial cells and immune regulation.

Immune response in macrophages and NK cells in endometriosis

Prior work has described the critical role of the immune system in maintaining endometrial homeostasis, with immune dysregulation contributing to endometrial pathology and pregnancy complications[50,51]. Given the heterogeneity of immune cells, we annotated the broad immune population into 11 distinct subsets using canonical immune cell markers: macrophages, monocytes, conventional type 1 dendritic cells (cDC1), plasmacytoid dendritic cells (pDCs), mast cells, uterine natural killer (NK) cells, innate lymphoid cells, plasma cells, stressed T cells[52], CD8+ T cells, T regulatory (Treg) cells. Additionally, a subset of lymphatic endothelial cells was observed to cluster with the immune cell population (**Fig. 5A,B**, **STable 2)**. The distribution of these cell types varied across disease conditions and menstrual phases (**SFig.**

330 **15A-C).** Additionally, the cell composition varied across patients and libraries **(SFig. 15D-E).** An
331 exploration of differential abundance revealed no significant differences between disease and
332 pristine control or among menstrual phases in immune cell populations (**SFig. 15F-G**).
333 Differential gene expression analysis of immune cell subsets identified macrophages,
334 NK cells and CD8+ T cells as the populations with the most transcriptomic differences between
335 endometriosis versus controls (**Fig. 5C, STable 12,13**). In the secretory phase, macrophages in
336 endometriosis eutopic endometrium samples exhibited upregulation of HSP genes related to
337 stress-induced damage protection (*HSPA1A* adj. p-val <0.001, log2FC = 2.17, *HSPA6* adj. p-val
338 < 0.001, log2FC = 2.32) and cytokine-related genes (*CXCL8*, adj. p-val < 0.05, log2FC = 0.93).
339 Additionally, macrophages in endometriosis showed downregulation of Class II HLA genes,
340 which encode human leukocyte antigen critical for immune recognition, in both the proliferative
341 (*HLA-DQA2*, adj. p-val < 0.001, log2FC = -0.34, *HLA-DRB5*, adj. p-val < 0.001, log2FC = -0.43)
342 and secretory phases (*HLA-DRB5*, adj. p-val < 0.001, log2FC=-1.13) (**Fig. 5D**). This
343 downregulation of HLA genes also occurred in conventional dendritic cells (cDC) during the
344 proliferative phase (*HLA-DRB5*, adj. p-val < 0.001, log2FC=-0.88; HLA-*DQA2* adj. p-val < 0.001,
345 log2FC=-1.2) (**STable 12**).
346 CD8+ T cells also exhibited transcriptional differences in endometriosis patients,
347 including upregulation of *TXNIP* (adj. p-val < 0.0001, log2FC=1.81) (**Fig. 5D**), which acts as a
348 regulator of cellular oxidation[53]. In addition, *XCL1* (adj. p-val < 0.0001, log2FC=-1.32), which is
349 expressed as part of the inflammatory response and *ISG15* (adj. P-val < 0.0001, log2FC=-0.71),
350 recognized for its immunomodulatory properties, were both downregulated in CD8+ T cells in
351 endometriosis, suggesting impaired immune surveillance.
352 NK cells exhibited many differences in both proliferative and secretory phases. In this
353 population, genes related to cytotoxic activity and chemokine-related recruitment of other
354 immune subsets (*GZMA* adj. p-val < 0.001, log2FC=-0.48, *GZMB* adj. p-val < 0.001, log2FC=-
355 0.34, *XCL1*, adj. p-val < 0.0001, log2FC=-1.06) were downregulated in cases during the

356 proliferative phase, while *TXNIP* was upregulated (adj. p-val < 0.001, log2FC=1.75) (**Fig. 5D,**
357 **STable12**). However no specific pathways were upregulated in the proliferative phase.

358 In the secretory phase, we detected overexpression of HSPs (*HSPA1A* adj. p-val <
359 0.001, log2FC=1.30, *HSPA6* adj. p-val < 0.001, log2FC=1.20). Notably, *GNLY*, which promotes
360 the induction of the immune response, was upregulated in this phase (adj. p-val < 0.01, log2FC
361 = 2.22), along with the cytotoxic gene *GZMB* (adj. p-val < 0.001, log2FC=2.19) (**Fig. 5D, Stable**
362 **12**). This pattern was also observed in the enrichment of pathways using GSEA, which showed
363 increased immune response and immune system processes in NK cells during the secretory
364 phase (**Fig. 5E, Stable 14**).Together, these findings suggest a specific impact of endometriosis
365 on uterine NK cell physiology during the secretory phase, which may not only affect fertility, but
366 also risks of pregnancy complications and tissue regeneration in the absence of pregnancy,
367 given the proposed roles of this specialized cell type.

368 Inferred communication between immune and non-immune cells in
369 endometriosis

370 To gain insight into the interplay between immune and non-immune cells, beyond
371 transcriptional changes. To explore this, we used CellChat[54] to compare cases versus pristine
372 controls, stratified by phase. Overall, we found distinct inferred receptor-ligand communication
373 patterns in both phases (**Fig. 6A**). In the proliferative phase, we identified a mix of upregulated
374 and downregulated pathways, including interactions exclusive to either cases or controls. In
375 contrast, in the secretory phase, we observed mainly upregulation of pathways in endometrium
376 from cases (**Fig. 6A**).

377 To investigate the most significant differences in communication pathways by cell type,
378 we visualized the top 10% differentially inferred pathways, stratified by phase. In the proliferative
379 phase, we observed that innate lymphoid cells (ILCs) exhibited the most significant

380 communication differences, characterized by decreased signaling to both immune and
381 nonimmune populations in cases (**Fig. 6B**). By identifying specific communication pathways, we
382 observed that ILCs in cases sent a decreased signal in TNF pathways (**Fig. 6C**). Further
383 analysis of ligand-receptor pairs in this population revealed that *TNFRSF1A* and *TNFRSF1B*
384 were only present in control samples (**SFig. 16**). While, TNF ligands are recognized for their role
385 in regulating inflammatory pathways in in endometriosis[55], it is hypothesized that increased
386 levels of soluble TNF receptors may serve as a regulatory mechanism to sequester and
387 neutralize TNF in various chronic inflammatory conditions[56]. Notably, TNFRSF1A has been
388 identified as a prospective therapeutic target for endometriotic lesions based on in vivo studies.
389 studies[57].

390 We performed a similar analysis in the secretory phase (**Fig. 6D**). VSM and stromal
391 fibroblasts exhibited the most upregulated interactions, acting as key ligand sources targeting
392 immune cells, including NK cells, CD8+ T cells, and macrophages. To investigate which
393 pathways where VSM were the sources of upregulation, we compared the differences in
394 signaling probability between cases and control samples (**Fig. 6E**). These highlighted the *THBS*
395 glycoprotein pathway and *FN1* pathway, both of which involve extracellular matrix (ECM)
396 proteins and interact with cell membrane receptors. Another important pathway was
397 *COLLAGEN*, with a presence in both controls and cases but significantly upregulated in
398 endometriosis. Collagen is an important ECM-interacting protein. One of its potential roles in
399 endometriosis is its deposition in endometriotic lesions as a result of chronic inflammation[58].
400 However, its mechanistic function in the endometrium of patients with the disease remains to be
401 determined.

402 # Discussion

403 Endometriosis is a prevalent and complex disease and understanding its impact on
404 different cell subtypes of the eutopic endometrium as its tissue of origin and as a target of
405 systemic associated with this disorder remains a challenge. It has been reported that eutopic
406 endometrium differs between individuals with and without endometriosis[59–61] .To investigate this,
407 we leveraged a comprehensive data set, containing over 235,000 cells encompassing people
408 with endometriosis, fibroids, and without disease across the menstrual cycle.

409 Studies have demonstrated that hormonal responses, especially to sex steroid
410 hormones during the menstrual cycle, affect endometrium and also endometriosis lesions[1,62,63].
411 This emphasizes the need to obtain and analyze samples by menstrual phases, and focus on
412 samples with no additional uterine/endometrial pathology and without exogenous hormonal
413 exposures[20]. By including samples spanning the menstrual cycle, avoiding hormonal
414 interventions, and incorporating pristine controls, we were able to minimize potential sources of
415 bias and better isolate disease-specific signals.

416 As we have shown previously[64], we established that the menstrual cycle phase
417 influences the epigenomic and transcriptomic endometrial landscapes. Herein, we have found
418 that specific cell types, such as fibroblasts and epithelial cells, contribute to endometrial
419 pathophysiology associated with endometriosis through mechanisms involving oxidative stress
420 and aberrant apoptosis signaling. We also demonstrated that alteration of immune cell
421 communication contributes to these processes. This study provides a valuable map of biological
422 pathways that characterize endometriosis in the eutopic endometrium across menstrual cycle
423 phases.

424 Building on this rationale, our study suggests that the differences between endometriosis
425 and controls are heavily dependent on cycle phase. Ours and other studies have demonstrated
426 that endometrial samples cluster more strongly by menstrual cycle phase than disease status at

427 molecular and epigenetic levels[61,65,66]. Consistent with these findings, our PCA revealed distinct
428 clustering related to the menstrual cycle phase independent of disease status. Furthermore, we
429 also showed consistent phase-specific differences at the pathway and transcriptomic levels
430 between endometriosis cases and fibroid controls, and pristine controls.

431 This phase-specific response is further supported by our observations of an increased
432 expression of heat shock protein (HSPs), especially HSP70-related isoforms[67], in secretory-
433 phase endometrial samples. HSP70 is considered a marker of oxidative stress in endometriosis
434 in lesions and in the eutopic endometrium[19,68]. HSPs influence inflammation pathways, resulting
435 in intrinsic apoptosis[69]. In fact, single-cell technology has identified HSPA6-related fibroblasts
436 with a pro-inflammatory phenotype in various tissues[25].

437 Several studies indicate elevated levels of HSPs in both eutopic and ectopic
438 endometrial tissues compared to controls[68,70–72], although the relative increase between these
439 tissues requires further research. The phase-specificity of this increase also remains
440 contentious, with some research suggesting phase-independent elevation, while others report a
441 rise specifically during the secretory phase[71,72]. Furthermore, differing mechanisms may underlie
442 this increase, depending on whether the tissue is eutopic or ectopic, and perhaps patient-level
443 factors that are unique to their history of environmental/medication exposures[70]. This pattern of
444 high HSP expression could be explained by the elevated reactive oxygen species, lower
445 antioxidant levels, and disrupted iron metabolism that occurs the in endometriosis disease
446 process. Endometrium from cases revealed that stromal fibroblasts and unciliated epithelia in
447 the secretory phase had elevated metal ion-related processes, accompanied by reduced
448 apoptosis signals, suggesting that endometrial cells may regulate ferroptosis susceptibility
449 through oxidative pathways to support growth and proliferation, as previously observed in
450 ectopic lesions [70,73,74].

451 Elevated oxidative expression was also present in specific cell types, including WFDC2+
452 fibroblasts, uterine NK cells, macrophages and ciliated cells. Previous studies have

453 demonstrated that macrophages secrete HSP70-inducing proinflammatory cytokines *in vitro* in
454 the context of other diseases[75], which was also observed in our results. Furthermore, this
455 oxidative pattern was consistent with *TXNIP* expression in uterine NK and $CD8^+$ T cells in
456 endometriosis samples. This expression is also required for the cleavage of HSP90[76],
457 potentially contributing to the pro-inflammatory microenvironment of endometrium in patients
458 with endometriosis[53,77,]. Another HSP-related response was the upregulation of CRYAB, which
459 was consistently upregulated in endometriosis across all broad cell populations in the secretory
460 phase. This gene has been implicated in cellular stress and also in decidualization[78,79].
461 Interestingly, therapies targeting oxidative stress have been proposed for the treatment
462 of endometriosis. Notably, TNFR1 signaling has emerged as a potential therapeutic
463 approach[70,80]. This is particularly compelling given our findings of TNFR1 downregulation in
464 endometriosis cases, as revealed by our cell–cell communication analysis.
465 The accumulation of HSPs in endometriosis also suggests cellular proliferation,
466 promoting the survival and implantation of cells at ectopic sites[81]. This pathologic implantation is
467 aided by reduced apoptosis in endometrial cells, allowing these cells to evade clearance
468 mechanisms and continue growing in ectopic lesions[82,83]. This is also confirmed by our finding of
469 increased negative regulation of cell death among fibroblasts, VSM and CE.
470 Besides enhanced cellular proliferation and reduced cell death, increased cell migration
471 is another potential mechanism for disease establishment originating in the eutopic
472 endometrium and continued growth of endometrial-like tissue ectopically. Notably, the aberrant
473 activation of Wnt/β-catenin pathway in the menstrual endometrium has been documented in
474 endometriosis patients and it may worsen the disease by increasing cell migration and invasion.
475 In our results we observed a consistent downregulation of *SFRP4* and *SFRP1*. These genes
476 inhibit Wnt signaling by preventing the interaction with WNT ligands[84]. The downregulation of
477 these inhibitors supports the abnormal activation of this pathway[22]. We also showed that WNT
478 regulation is decreased at the pathway level in EMT1 cells.

479 In our analysis, we identified two distinct EMT populations. One cell population exhibited
480 mesenchymal and epithelial markers (EMT1). By contrast, the second EMT population showed
481 expression of *VIM*+ as a marker (EMT2). Notably, during the secretory phase, EMT1 population
482 showed increased cell migration, locomotion, cell motility, and cell adhesion in endometriosis.
483 These findings align with previous research indicating that EMT is an important pathogenic
484 mechanism, by losing its polarized cytoskeletal organization and cell-to-cell connections and
485 increasing motility[85,86]. EMTs are stimulated by estrogen levels and hypoxia signals in eutopic
486 and ectopic endometrium[86,87], consistent with our finding of high oxidative stress. Additionally, a
487 key regulation of EMT mobility, vimentin, was downregulated in this population. This
488 encourages further exploration, as previous studies have reported conflicting results regarding
489 the significance of VIM and other key EMT markers[86,88–90], showing differences between eutopic
490 and ectopic endometrium for master EMT genes[88].
491 Cell migration is significantly influenced by the dynamic interactions between cells and
492 their extracellular matrix (ECM)[91]. Aberrant expression of ECM-related factors was shown in our
493 cell-cell communication analysis, with ECM interactions upregulated in VSM, including ligands
494 for collagen and FN1. Furthermore, in the proliferating fibroblast population, we observed an
495 upregulation in CCN2, which coordinates key components of the ECM, tissue repair, and growth
496 factors[92]. This highlights the significance of ECM-related genes in endometriosis[45,93,94]. This was
497 also shown by the upregulation of *MMP7* in glandular epithelia. MMPs in endometriosis could
498 influence processes such as invasion, angiogenesis, inflammation and fibrosis, and are
499 exacerbated by oxidative stress[89,95].
500 The role of immune cells in endometriosis is pivotal for the disease's progression, for
501 example, through their interactions with non-immune tissue types. This was also observed in
502 endothelial cells, where leukocyte migration was upregulated, along with genes related to this
503 process for example *ICAM1*[96]. This process is essential for the induction, maintenance, and
504 regulation of immune responses and can be influenced by cytokine expression, which affects

505 the functionality of other cell types in preparing for and sustaining pregnancy, as well as
506 maintaining overall tissue homeostasis.

507 Another critical component in the progression and clinical management of endometriosis
508 is immune surveillance and regulating inflammatory response. Immune recognition is influenced
509 by MHC class II molecules, expressed by antigen-presenting cells like macrophages, which are
510 encoded by HLA genes that bind various peptides[97]. Our results show a reduction in *HLA-DR*
511 expression in the macrophage and cDC populations in cases, indicating a functional impairment
512 in antigen-presenting cells. This reduction was also found in previous studies of women with
513 infertility, both with and without endometriosis[98]. Further research is needed regarding the role
514 of the HLA system in this disease[99]. We also observed downregulation of chemokine *XCL1* in
515 CD8+ T cells and NK cells in the proliferative phase, which play a critical role in recruiting other
516 immune cell types such as DCs[100].

517 Interestingly, we found contradictory expressions of specific cytotoxic molecules in NK
518 cells, including upregulation of *GNLY* in the secretory phase and phase-specific expression of
519 *GZMB* in samples from cases versus controls. The change in expression of these genes in
520 endometriosis has been debated, with evidence for both downregulation and upregulation[101,102].
521 The observed upregulation of *GNLY* could be due to the inflammatory conditions of the
522 endometrium. Conversely, the downregulation of *GZMB* and *GZMA* could suggest blunted NK
523 cell activity, which may facilitate the progression of endometriosis. In general, this result
524 highlights how endometriosis involves a complex interplay of inhibitors and activators.

525 An unexpected finding was the upregulation of *PAEP* in endometriosis samples, also
526 known as glycodelin (Gd) in endometrial epithelial cells. Gd is thought to be involved in
527 establishing endometrial receptivity and is considered a biomarker of the window of
528 implantation[103,104]. Single-cell analysis further associated *PAEP* expression with a distinct
529 epithelial sub-cluster found exclusively in control samples, opening the window of implatantion[15].
530 However, studies have also shown mixed results regarding Gd levels, with some reporting

531 elevated serum levels linked to disease infiltration, while others found only minor differences in
532 expression between control and endometriosis[105–108]. In our analysis, this gene was persistently
533 upregulated in endometriosis samples in both proliferative and secretory phases in the
534 unciliated epithelial population. We propose that this acyclic, constitutive expression may reflect
535 dysregulation of this receptivity marker and immune modulator in the eutopic endometrium,
536 making it unfavorable for embryo implantation. Discrepancies among multiple studies may be
537 attributed to variations in sampling time points. Gd expression fluctuates throughout the
538 menstrual cycle, peaking during implantation. However, in endometriosis, altered progesterone
539 response could lead to a different pattern of Gd expression, potentially causing fertility issues[109].
540 Future research focusing on more precise time points of the menstrual cycle could help answer
541 these questions.

542 In this study, we present a wide-ranging analysis of patients with endometriosis,
543 alongside patients with uterine fibroids and pristine controls. Although our pristine controls
544 (ovum donors not undergoing ovarian stimulation) did not undergo surgical confirmation to rule
545 out endometriosis, it is important to note that they had no history of gynecologic disorders or
546 symptoms of endometriosis.

547 While we expand upon previous studies by including samples from both the proliferative
548 and secretory phases, the current study's limited sample size may restrict the ability to detect
549 subtle phase-specific changes. Including additional time points to create a more continuous map
550 of the menstrual cycle, as well as a better representation of the late and early proliferative and
551 secretory phases, would strengthen our findings. We found limited detection of differential
552 abundance across cell types. We suggest increasing the sample size, especially for these time
553 points not captured, which would provide greater statistical power. Additionally, while the
554 inclusion of multiple endometriosis stages could help characterize the disease, the
555 heterogeneity of sample stages and types may complicate the identification of specific
556 differences between endometriosis variants.

557 Overall, our results highlight the importance of oxidative stress, apoptosis, and
558 extracellular matrix organization as potential contributors to the pathophysiology of endometrial
559 dysfunction in endometriosis patients. Additionally, we have identified key players such as EMT
560 cells, specific endometrial fibroblast populations, and altered communication in NK cells and
561 macrophages in this disease. These discoveries enhance our understanding of the complex
562 interplay in the eutopic endometrial microenvironment in patients with endometriosis. Moreover,
563 we provide multiple comparative analyses, examining not only the differences between
564 endometriosis and healthy controls but also considered various stages of endometriosis and
565 fibroid controls. We observed a notable similarity between fibroids and endometriosis,
566 underscoring the critical importance of utilizing robust control groups.

567 Furthermore, understanding these eutopic alterations is crucial not only for the
568 pathogenesis of lesions but also for helping patients experiencing fertility problems. Identifying
569 transcriptomic signatures in eutopic endometrium could pave the way for less invasive
570 diagnostic approaches to endometriosis. For example, our data could contribute to novel
571 diagnostic strategies through transcriptomic prediction and drug interaction studies, and it could
572 be leveraged for the development of targeted mono- or multi-modal therapies. We believe this
573 study represents a valuable resource that serves as an atlas to better understand the impact of
574 endometriosis, particularly on the eutopic endometrium.

575 Methods and Materials

576 Subject details

577 This study was conducted in accordance with the Institutional Review Board (IRB) guidelines of
578 the University of California, San Francisco under an approved IRB protocol (#10-02786) and in
579 accordance with the Declaration of Helsinki. Informed written consent was obtained from all

580 subjects before endometrial tissue sampling. Subjects were 20-45 years old with regular
581 menstrual cycles (28–30 days) and body mass index 19–29 kg m2 (inclusive) (**STable 1**).
582 Cases included subjects with rASRM stages I-IV, endometriomas, superficial, and/or deep
583 infiltrating disease diagnosed at surgery and confirmed histologically. Controls included samples
584 from subjects without endometriosis but undergoing surgery for symptomatic uterine fibroids/
585 leiomyoma, a common condition of reproductive aged women[110] ("pathologic controls") and from
586 healthy ovum donor volunteers ("pristine controls"). Subjects were excluded if they had used
587 hormonal contraception or GnRH analogue less than 3 months prior to sampling, had polycystic
588 ovary syndrome, and reproductive tract infections or malignancies. Some endometriosis cases
589 additionally presented adenomyosis, fibroids, or uterine polyps (**STable1**). Cycle phase was
590 determined by endometrial histology[111], serum estradiol and progesterone levels, and last
591 menstrual period. Biospecimens were obtained and processed according to the UCSF Uterine
592 Disorders Tissue Biorepository standard operating procedures[112].

593 Endometrium tissue dissociation, cryopreservation, and epithelial cell 594 enrichment.

595 A two-stage dissociation protocol was used to dissociate endometrial tissue and separate it into
596 stromal- and epithelial-enriched single-cell suspensions. Undissociated endometrial tissue was
597 rinsed with PBS (Sigma) to remove blood and mucus. Rinsed tissue was minced into the
598 smallest possible pieces (~1×1×1 mm) with disposable scalpels on a petri dish and dissociated
599 in collagenase I or IV (Sigma) at 37 °C for 1hr in a 15 ml Falcon tube with constant agitation on
600 a Nutator. This primary enzymatic step dissociates stromal cells into single cells while leaving
601 epithelial glands and lumen mostly undigested. At this stage, the epithelial portion was either
602 separated from the stromal cells via a 40-µm cell strainer or left undigested within the stromal
603 cells. If present, red blood cells were lysed with 1× RBC Lysis Buffer (Invitrogen). The resulting

604 suspensions were then cryopreserved using DMSO-based cryoprotectant (80% DMEM, 10%
605 serum, 10% DMSO) following standard protocol.

606 The supernatant was therefore collected as the stromal fibroblast-enriched suspension. The
607 epithelial pellet was dissociated in 1 ml Accutase (Millipore) for 30 min at 37 °C, during which
608 homogenization was performed every 15 minutes via intermittent pipetting using a 1mL pipette.
609 DNaseI (Roche) was then added to the solution to a final concentration of 0.2mg/mL to digest
610 extracellular genomic DNA and was quenched with 9 ml of DMEM after 1 min of incubation at
611 room temperature. The resulting cell suspension was pipetted, filtered through a 40-μm cell
612 strainer, and centrifuged at 300 RFC for 5 min. The pellet was resuspended as the epithelium-
613 enriched suspension.

614 Sample multiplexing and randomization

615 Multiplexing via natural genetic variants[113] was used for single-cell capture, cDNA generation,
616 and library preparation. Briefly, samples from 4 different individuals were pooled and loaded
617 onto a single well of the Chromium Next GEM Chip G (10x Genomics). For demultiplexing, an
618 aliquot of each sample was analyzed separately by bulk RNAseq to associate high-confidence
619 genetic variation with individual samples of origin.

620 For multiplexing, stratified randomization[114] was used to create groups of 4 individuals to
621 balance the influence of the following covariates: conditions (pristine controls, pathological
622 controls, stage I-II endometriosis, stage III-IV) and menstrual cycle phase (proliferative,
623 secretory). Briefly, samples were classified into categories based on the combination of the
624 covariates above. A random number between 1~n (n=desired number of groups) was assigned
625 to each sample in each of the categories, with 4 being the maximum number of samples per
626 group, such that each sample was assigned to n groups of 4 samples.

627 ## Single-cell sequencing

628 *Single-cell capture, cDNA generation, and library preparation via Chromium 10x platform and*
629 *chemistry.* A total of ~60,000 cells from four individuals (~15,000 cells/each) were loaded onto a
630 single well of the Chromium Next GEM Chip G (10x Genomics). GEM generation and barcoding,
631 reverse transcription, cDNA generation, and library construction were performed following the
632 manufacturer's protocol (Single cell 3′ reagent kit v.3.1, 10x Genomics). Specifically, 11 PCR
633 cycles were used for cDNA generation, whereas 11-13 cycles were used for PCR during library
634 preparation, depending on the amount of cDNA input and the manufacturer's guidelines.

635 *Bulk RNA extraction, cDNA generation, and library preparation.* For each sample, bulk RNA
636 extraction was performed on ~100,000 cells using AllPrep DNA/RNA Microkit and protocol
637 Simultaneous Purification of Genomic DNA and Total RNA from Animal and Human cells
638 (Qiagen). The resulting RNA was diluted and quantified via Nanodrop and Fragment analyzer.
639 1.5ng total RNA with RIN>8 was used for cDNA generation using SMARTseq v4 chemistry
640 (Takara) and library prepped using Nextera DNA Flex Library Preparation Kit (Illumina, San
641 Diego, CA).

642 *Sequencing*. Single-cell libraries were sequenced to a depth of ~25,000 reads per cell on a
643 Novaseq. Bulk RNAseq libraries were sequenced to a depth of ~30M reads per sample on a
644 HiSeq.

645 ## Single-cell data processing and filtering

646 Thirteen libraries were independently processed using the Cell Ranger[115] software pipeline
647 (version 3.1.0). Reads were mapped to the transcriptome using the human hg38 version, and
648 UMI counts were calculated using default parameters. The samples were demultiplexed using

649 Freemuxlet[113] using the number of samples per pool and a list of valid barcodes. We processed
650 each UMI count matrix using the R package Seurat (v.4.0.3)[116]. Using Freemuxlet cells were
651 classified according to their UMI content and doublets, and ambiguous cells were filtered, while
652 singlets were retained. Further filtering per each pool included removing cells with high
653 mitochondrial content (>20%), high ribosomal content (>50%), high RNA count (50,000>), low
654 feature (<200) and low RNA count (<300). We performed normalization and scaling. We
655 calculated variable features, principal component analysis (PCA), and ran UMAP and clustering
656 (Leiden). To assign demultiplexed cells to the sample of origin, genetic profiles between
657 demultiplexed cells and bulk RNA profiles were compared using bcftools (v.1.10). Before
658 integration we performed a second filtering step, we removed clusters which top markers were
659 mitochondrial genes. We employed Seurat to combine the data from the 13 pools into a single
660 object. During this process, mitochondrial, ribosomal, and cell cycle scores were regressed out
661 during scaling. To correct batch effects, we utilized Harmony[117] to perform pool integration.
662 Subsequently, we conducted PCA on the variable genes (n=3000), and it was used as input for
663 an unsupervised cell clustering approach using the Louvain algorithm. Dimensionality reduction
664 and visualization were performed using UMAP. One individual using hormonal medication was
665 removed after clustering. Following cell filtering, the single-cell dataset consisted of 228,021
666 cells with 29,001 genes expressed. (**STable 1**).
667

668 Identification of cell types

669 Broad cell types were classified through a combination of manual and automated annotation.
670 Cell type-specific markers were identified using the FindMarkers function in Seurat with default
671 parameters. Additionally, clusters exhibiting high mitochondrial gene expression among their top
672 10 markers were excluded from further analysis. Subsequently, the remaining cells were re-

673 clustered. This process was repeated until the top 10 markers for every cluster were not part of
674 the mitochondrial family.

675 For reference annotations, a previous dataset of the human endometrium was utilized[118].
676 This dataset was downloaded, checked for quality, and their labels verified. This dataset was
677 then used as reference using SingleR[119] for automated annotation of our broad main cell types.
678 This annotation was cross-referenced with the top gene markers.

679 *Identification of fine cell types.* Epithelial, stromal, and immune subpopulations were
680 identified using a tailored approach with Seurat's FindNeighbors and FindClusters functions.
681 Each cell type was analyzed at a resolution parameter adjusted according to its heterogeneity.
682 Identification of specific markers was subsequently performed using the FindMarkers function in
683 Seurat with default parameters. Clusters expressing mitochondrial genes (MT) among their top
684 10 markers, or immune-specific genes in non-immune cell types, were excluded. The cells were
685 then re-clustered. This process was repeated multiple times for epithelial cells until no clusters
686 with high MT expression remained. Manual annotation of the identified clusters was conducted
687 based on markers described in the literature. The result of these subsets were consequentially
688 used for downstream analysis, for broad and specific cell types.

689 *Fibroblast Fine Annotation:* After re-clustering, we obtained seven fibroblast clusters and
690 the previously reported vascular smooth muscle (VSM) cluster. We identified Cluster 0 (C0) with
691 marker S100A4, described as an activated fibroblast[120]; C1 with IGF1+ expression, indicating
692 decidualization[121]; C2 with HSP markers, suggesting stress; C3 with SFRP4+ expression, a
693 previously described cluster[23]; Cluster C4 with matrix metalloproteinase (MMP) genes related to
694 the extracellular matrix[122]; C5 with TOP2A+ expression, a proliferative marker[123,124]; C6
695 expressing VSM markers; and C7 with WAP four-disulfide core domain 2 (WFC2) expression.

696 *Epithelial Fine annotation:* After re-clustering, we obtained eight epithelial clusters. We
697 identified C1 assigned as EMT epithelia with expression of collagen markers[125,126], C3 with

698 expression of vimentin (VIM) and SOX4[127,128]; C4 with ciliated epithelial markers PIFO+, and C7
699 with expression of MUC5B+/TFF3+ indicating progenitor cells[14].
700

701 Differential abundance, PCA composition, differential gene expression
702 and pathway analysis

703 Differential abundance in each specific cell type was assessed using t-test and
704 compare_means, provided by the package ggpubr (v 0.6.0) resulting in adjusted p-values per
705 each menstrual phase or disease comparison.
706 PCA composition was obtained by calculating the ratio of each specific cell type
707 compared to the corresponding broad cell type for every sample. This was done for stromal,
708 epithelial and immune subsets.
709 Differential gene expression analyses were conducted using the FindMarkers function in
710 Seurat with the method MAST[129] (v. 1.18). The covariates associated with de-identified patient
711 ID and library prep were included, and p-values were adjusted using the Benjamini-Hochberg
712 method. DGE between endometriosis and pristine controls was performed in cell populations
713 with two or more controls. Broad cell types and specific cell types were analyzed, using single-
714 cell objects after filtering and sub-setting (see above) for immune, stromal fibroblast, VSM,
715 ciliated and unciliated epithelial cells. Endothelia cells analysis was performed based on object
716 containing all cells.
717 For pathway analysis, genes with an adjusted p-value less than 0.05 were selected. To
718 calculate enrichment in GSEA we used clusterProfiler[130], using “BP” as ontology, with pathways
719 chosen based on a Benjamini-Hochberg adjusted p-value threshold less than 0.05.
720

721 ## Cell communication analysis

722 In silico communication analysis was performed with CellChat[54] (v1.6.1) using the
723 CellChatDB.human as the database and populations as previously defined as broad non-
724 immune (Stromal Fibroblast, VSM, Unicliated Epithelia, Ciliated Epithelia, and Endothelia) and
725 broad immune. Each category (proliferative endometriosis, proliferative control, secretory
726 endometriosis, and secretory control) was processed independently. Following standard
727 procedures, we computed Communication Probability and filtered cell-cell communication with
728 less than 10 cells. Cell objects were then merged and compared, stratifying by menstrual cycle.
729 Data for visualization was retrieved by using the function subsetCommunication.

730 ## Data Availability

731 Data available in CZ cellxgene (https://cellxgene.cziscience.com/). ScRNA-seq datasets to
732 reproduce all figures, can be accessed and downloaded through the web portal.

733 ## Code availability

734 The code for clustering, annotation, downstream analyses (including differential gene
735 expression, differential abundance, and pathway enrichment), as well as generating figures, is
736 available on GitHub https://github.com/almonteloya/Endometriosis_sc

737 ## References

738 1. Giudice, L. C. & Kao, L. C. Endometriosis. *The Lancet* **364**, 1789–1799 (2004).
739 2. Zondervan, K. T., Becker, C. M. & Missmer, S. A. Endometriosis. *N. Engl. J. Med.* **382**,
740 1244–1256 (2020).

741 3. Zondervan, K. T. *et al.* Endometriosis. *Nat. Rev. Dis. Primer* **4**, 9 (2018).
742 4. Giudice, L. C., Oskotsky, T. T., Falako, S., Opoku-Anane, J. & Sirota, M. Endometriosis in
743 the era of precision medicine and impact on sexual and reproductive health across the
744 lifespan and in diverse populations. *FASEB J.* **37**, e23130 (2023).
745 5. Dymanowska-Dyjak, I. *et al.* Immune Dysregulation in Endometriomas: Implications for
746 Inflammation. *Int. J. Mol. Sci.* **25**, 4802 (2024).
747 6. The World Bank. Population ages 15- 64 (% of population). (2017).
748 7. Simoens, S. *et al.* The burden of endometriosis: costs and quality of life of women with
749 endometriosis and treated in referral centres. *Hum. Reprod.* **27**, 1292–1299 (2012).
750 8. Taylor, H. S., Kotlyar, A. M. & Flores, V. A. Endometriosis is a chronic systemic disease:
751 clinical challenges and novel innovations. *The Lancet* **397**, 839–852 (2021).
752 9. Giudice, L. C., Irwin, J. C. & Liu, B. Endometriosis and adenomyosis unveiled through
753 single-cell glasses. *Press* (2024).
754 10. Ponnampalam, A. P., Weston, G. C., Trajstman, A. C., Susil, B. & Rogers, P. A. W.
755 Molecular classification of human endometrial cycle stages by transcriptional profiling.
756 *MHR Basic Sci. Reprod. Med.* **10**, 879–893 (2004).
757 11. Talbi, S. *et al.* Molecular Phenotyping of Human Endometrium Distinguishes Menstrual
758 Cycle Phases and Underlying Biological Processes in Normo-Ovulatory Women.
759 *Endocrinology* **147**, 1097–1121 (2006).
760 12. Garcia-Alonso, L. *et al.* Mapping the temporal and spatial dynamics of the human
761 endometrium in vivo and in vitro. *Nat. Genet.* **53**, 1698–1711 (2021).
762 13. Ma, J. *et al.* Single-cell transcriptomic analysis of endometriosis provides insights into
763 fibroblast fates and immune cell heterogeneity. *Cell Biosci.* **11**, 125 (2021).
764 14. Fonseca, M. A. S. *et al.* Single-cell transcriptomic analysis of endometriosis. *Nat. Genet.*
765 **55**, 255–267 (2023).

766 15. Huang, X. *et al.* Single-cell transcriptome analysis reveals endometrial immune
767 microenvironment in minimal/mild endometriosis. *Clin. Exp. Immunol.* **212**, 285–295
768 (2023).
769 16. Shih, A. J. *et al.* Single-cell analysis of menstrual endometrial tissues defines phenotypes
770 associated with endometriosis. *BMC Med.* **20**, 315 (2022).
771 17. Tan, Y. *et al.* Single-cell analysis of endometriosis reveals a coordinated transcriptional
772 programme driving immunotolerance and angiogenesis across eutopic and ectopic tissues.
773 *Nat. Cell Biol.* **24**, 1306–1318 (2022).
774 18. American Society For Reproductive Medicine. Revised American Society for Reproductive
775 Medicine classification of endometriosis: 1996. *Fertil. Steril.* **67**, 817–821 (1997).
776 19. Lambrinoudaki, I. V. *et al.* Measurable serum markers of oxidative stress response in
777 women with endometriosis. *Fertil. Steril.* **91**, 46–50 (2009).
778 20. Ahn, S. H., Singh, V. & Tayade, C. Biomarkers in endometriosis: challenges and
779 opportunities. *Fertil. Steril.* **107**, 523–532 (2017).
780 21. Hu, C. *et al.* Heat shock proteins: Biological functions, pathological roles, and therapeutic
781 opportunities. *MedComm* **3**, e161 (2022).
782 22. Matsuzaki, S., Botchorishvili, R., Pouly, J. L. & Canis, M. Targeting the Wnt/β-catenin
783 pathway in endometriosis: a potentially effective approach for treatment and prevention.
784 *Mol. Cell. Ther.* **2**, 36 (2014).
785 23. Wu, B. *et al.* SFRP4+ stromal cell subpopulation with IGF1 signaling in human endometrial
786 regeneration. *Cell Discov.* **8**, 95 (2022).
787 24. Yildiz, S. *et al.* Adenomyosis: single-cell transcriptomic analysis reveals a paracrine
788 mesenchymal–epithelial interaction involving the WNT/SFRP pathway. *Fertil. Steril.* **119**,
789 869–882 (2023).
790 25. Gao, Y. *et al.* Cross-tissue human fibroblast atlas reveals myofibroblast subtypes with
791 distinct roles in immune modulation. *Cancer Cell* **42**, 1764-1783.e10 (2024).

792 26. Cheong, M.-L., Lai, T.-H. & Wu, W.-B. Connective tissue growth factor mediates
793 transforming growth factor β-induced collagen expression in human endometrial stromal
794 cells. *PLOS ONE* **14**, e0210765 (2019).
795 27. Zhang, X., Zhang, X., Huang, W. & Ge, X. The role of heat shock proteins in the regulation
796 of fibrotic diseases. *Biomed. Pharmacother.* **135**, 111067 (2021).
797 28. Yang, D., Liu, J., Qian, H. & Zhuang, Q. Cancer-associated fibroblasts: from basic science
798 to anticancer therapy. *Exp. Mol. Med.* **55**, 1322–1332 (2023).
799 29. Sun, C. *et al.* Transgelin promotes lung cancer progression via activation of cancer-
800 associated fibroblasts with enhanced IL-6 release. *Oncogenesis* **12**, 18 (2023).
801 30. Chen, S.-T. *et al.* Embryo-derive TNF promotes decidualization via fibroblast activation.
802 *eLife* **12**, e82970 (2023).
803 31. Shi, J., Jing, W., He, Y. & Huang, Y. Decreased expression of KLF6 in ectopic endometrial
804 stromal cells contributes to endometriosis progression by targeting CTNNB1. *Cell. Signal.*
805 **120**, 111230 (2024).
806 32. Sureshbabu, A. *et al.* IGFBP-5 induces epithelial and fibroblast responses consistent with
807 the fibrotic response. *Biochem. Soc. Trans.* **37**, 882–885 (2009).
808 33. McTavish, N., Copeland, L. A., Saville, M. K., Perkins, N. D. & Spruce, B. A. Proenkephalin
809 assists stress-activated apoptosis through transcriptional repression of NF-κB- and p53-
810 regulated gene targets. *Cell Death Differ.* **14**, 1700–1710 (2007).
811 34. Chathuranga, W. A. G. *et al.* Gadd45β is critical for regulation of type I interferon signaling
812 by facilitating G3BP-mediated stress granule formation. *Cell Rep.* **42**, 113358 (2023).
813 35. National Center for Biotechnology Information. TCIM transcriptional and immune response
814 regulator [Homo sapiens (human)].
815 36. Moon, Y.-M. *et al.* The Fos-Related Antigen 1–JUNB/Activator Protein 1 Transcription
816 Complex, a Downstream Target of Signal Transducer and Activator of Transcription 3,

817 Induces T Helper 17 Differentiation and Promotes Experimental Autoimmune Arthritis.
818 *Front. Immunol.* **8**, 1793 (2017).
819 37. Younesi, F. S., Miller, A. E., Barker, T. H., Rossi, F. M. V. & Hinz, B. Fibroblast and
820 myofibroblast activation in normal tissue repair and fibrosis. *Nat. Rev. Mol. Cell Biol.* **25**,
821 617–638 (2024).
822 38. Łuszczyński, K. *et al.* Surface Molecular Markers for the Isolation of Viable Fibroblast
823 Subpopulations in the Female Reproductive Tract: A Comprehensive Review. *Int. J. Mol.*
824 *Sci.* **26**, 233 (2024).
825 39. Zhan, Y. *et al.* Human epididymis protein 4 aggravates airway inflammation and
826 remodeling in chronic obstructive pulmonary disease. *Respir. Res.* **23**, (2022).
827 40. LeBleu, V. S. *et al.* Identification of human epididymis protein-4 as a fibroblast-derived
828 mediator of fibrosis. *Nat. Med.* **19**, 227–231 (2013).
829 41. Dong, L., Li, Y., Song, X., Sun, C. & Song, X. SFRP1 mediates cancer-associated
830 fibroblasts to suppress cancer cell proliferation and migration in head and neck squamous
831 cell carcinoma. *BMC Cancer* **24**, 1165 (2024).
832 42. Saegusa, M., Hashimura, M. & Kuwata, T. Sox4 functions as a positive regulator of β-
833 catenin signaling through upregulation of TCF4 during morular differentiation of
834 endometrial carcinomas. *Lab. Invest.* **92**, 511–521 (2012).
835 43. Zutautas, K. B. *et al.* The dysregulation of leukemia inhibitory factor and its implications for
836 endometriosis pathophysiology. *Front. Immunol.* **14**, 1089098 (2023).
837 44. Figula, J., Baran, R. M. & Jach, R. Osteopontin as a marker of endometriosis — the
838 current state of knowledge. *Ginekol. Pol.* VM/OJS/J/86232 (2023) doi:10.5603/gpl.86232.
839 45. Ke, J., Ye, J., Li, M. & Zhu, Z. The Role of Matrix Metalloproteinases in Endometriosis: A
840 Potential Target. *Biomolecules* **11**, 1739 (2021).

841 46. Kutsukake, M. *et al.* Circulating IGF-binding protein 7 (IGFBP7) levels are elevated in
842 patients with endometriosis or undergoing diabetic hemodialysis. *Reprod. Biol. Endocrinol.*
843 **6**, 54 (2008).
844 47. Chen, L., Hui, L. & Li, J. The multifaceted role of insulin-like growth factor binding protein 7.
845 *Front. Cell Dev. Biol.* **12**, 1420862 (2024).
846 48. Vargas, E. *et al.* The mid-secretory endometrial transcriptomic landscape in endometriosis:
847 a meta-analysis. *Hum. Reprod. Open* **2022**, hoac016 (2022).
848 49. Nothnick, W. B. *et al.* Macrophage Migration Inhibitory Factor Receptor, CD74, is
849 Overexpressed in Human and Baboon (Papio Anubis) Endometriotic Lesions and
850 Modulates Endometriotic Epithelial Cell Survival and Interleukin 8 Expression. *Reprod. Sci.*
851 **25**, 1557–1566 (2018).
852 50. Zhang, T., De Carolis, C., Man, G. C. W. & Wang, C. C. The link between immunity,
853 autoimmunity and endometriosis: a literature update. *Autoimmun. Rev.* **17**, 945–955
854 (2018).
855 51. Vallvé-Juanico, J., Houshdaran, S. & Giudice, L. C. The endometrial immune environment
856 of women with endometriosis. *Hum. Reprod. Update* **25**, 565–592 (2019).
857 52. Chu, Y. *et al.* Pan-cancer T cell atlas links a cellular stress response state to
858 immunotherapy resistance. *Nat. Med.* **29**, 1550–1562 (2023).
859 53. Choi, E.-H. & Park, S.-J. TXNIP: A key protein in the cellular stress response pathway and
860 a potential therapeutic target. *Exp. Mol. Med.* **55**, 1348–1356 (2023).
861 54. Jin, S. *et al.* Inference and analysis of cell-cell communication using CellChat. *Nat.*
862 *Commun.* **12**, 1088 (2021).
863 55. Wu, M. & Ho, H. The Role of Cytokines in Endometriosis*. *Am. J. Reprod. Immunol.* **49**,
864 285–296 (2003).
865 56. Rojas-Cartagena, C., Appleyard, C. B., Santiago, O. I. & Flores, I. Experimental Intestinal
866 Endometriosis Is Characterized by Increased Levels of Soluble TNFRSF1B and

867 Downregulation of Tnfrsf1a and Tnfrsf1b Gene Expression1. *Biol. Reprod.* **73**, 1211–1218
868 (2005).
869 57. D'Hooghe, T. M. *et al.* Recombinant Human TNFRSF1A (r-hTBP1) Inhibits the
870 Development of Endometriosis in Baboons: A Prospective, Randomized, Placebo- and
871 Drug-Controlled Study1. *Biol. Reprod.* **74**, 131–136 (2006).
872 58. Colgrave, E. M. *et al.* Distribution of smooth muscle actin and collagen in superficial
873 peritoneal endometriotic lesions varies from the surrounding microenvironment. *Reprod.*
874 *Biomed. Online* **48**, 103610 (2024).
875 59. Benagiano, G., Brosens, I. & Habiba, M. Structural and molecular features of the
876 endomyometrium in endometriosis and adenomyosis. *Hum. Reprod. Update* **20**, 386–402
877 (2014).
878 60. Liu, H. & Lang, J. H. Is abnormal eutopic endometrium the cause of endometriosis? The
879 role of eutopic endometrium in pathogenesis of endometriosis. *Med. Sci. Monit.* **17**, RA92–
880 RA99 (2011).
881 61. Houshdaran, S. *et al.* Aberrant Endometrial DNA Methylome and Associated Gene
882 Expression in Women with Endometriosis. *Biol. Reprod.* **95**, 93–93 (2016).
883 62. Kuan, K. K. W., Gibson, D. A., Whitaker, L. H. R. & Horne, A. W. Menstruation
884 Dysregulation and Endometriosis Development. *Front. Reprod. Health* **3**, 756704 (2021).
885 63. Chantalat, E. *et al.* Estrogen Receptors and Endometriosis. *Int. J. Mol. Sci.* **21**, 2815
886 (2020).
887 64. Houshdaran, S., Zelenko, Z., Irwin, J. C. & Giudice, L. C. Human Endometrial DNA
888 Methylome Is Cycle-Dependent and Is Associated With Gene Expression Regulation. *Mol.*
889 *Endocrinol.* **28**, 1118–1135 (2014).
890 65. Mortlock, S. *et al.* Global endometrial DNA methylation analysis reveals insights into mQTL
891 regulation and associated endometriosis disease risk and endometrial function. *Commun.*
892 *Biol.* **6**, 780 (2023).

893 66. Saare, M. *et al.* The influence of menstrual cycle and endometriosis on endometrial
894 methylome. *Clin. Epigenetics* **8**, 2 (2016).
895 67. Stricher, F., Macri, C., Ruff, M. & Muller, S. HSPA8/HSC70 chaperone protein: Structure,
896 function, and chemical targeting. *Autophagy* **9**, 1937–1954 (2013).
897 68. Matsuzaki, S. & Schubert, B. Oxidative stress status in normal ovarian cortex surrounding
898 ovarian endometriosis. *Fertil. Steril.* **93**, 2431–2432 (2010).
899 69. Ikwegbue, P., Masamba, P., Oyinloye, B. & Kappo, A. Roles of Heat Shock Proteins in
900 Apoptosis, Oxidative Stress, Human Inflammatory Diseases, and Cancer. *Pharmaceuticals*
901 **11**, 2 (2017).
902 70. Clower, L., Fleshman, T., Geldenhuys, W. J. & Santanam, N. Targeting Oxidative Stress
903 Involved in Endometriosis and Its Pain. *Biomolecules* **12**, 1055 (2022).
904 71. Tabibzadeh, S., Kong, Q. F., Satyaswaroop, P. G. & Babaknia, A. Heat shock proteins in
905 human endometrium throughout the menstrual cycle. *Hum. Reprod.* **11**, 633–640 (1996).
906 72. Ota, H., Igarashi, S., Hatazawa, J. & Tanaka, T. Distribution of heat shock proteins in
907 eutopic and ectopic endometrium in endometriosis and adenomyosis. *Fertil. Steril.* **68**, 23–
908 28 (1997).
909 73. Scutiero, G. *et al.* Oxidative Stress and Endometriosis: A Systematic Review of the
910 Literature. *Oxid. Med. Cell. Longev.* **2017**, 7265238 (2017).
911 74. Li, Y. *et al.* Double-edged roles of ferroptosis in endometriosis and endometriosis-related
912 infertility. *Cell Death Discov.* **9**, 306 (2023).
913 75. Smith, K. J. *et al.* Heat shock protein 70B' (HSP70B') expression and release in response
914 to human oxidized low density lipoprotein immune complexes in macrophages. *J. Biol.*
915 *Chem.* **285**, 15985–15993 (2010).
916 76. Park, S. *et al.* Contribution of HSP90 Cleavage to the Cytotoxic Effect of Suberoylanilide
917 Hydroxamic Acid *In Vivo* and the Involvement of TXNIP in HSP90 Cleavage. *Biomol. Ther.*
918 **32**, 115–122 (2024).

919 77. Mohamed, I. N., Li, L., Ismael, S., Ishrat, T. & El-Remessy, A. B. Thioredoxin interacting
920 protein, a key molecular switch between oxidative stress and sterile inflammation in cellular
921 response. *World J. Diabetes* **12**, 1979–1999 (2021).
922 78. Zuo, R.-J. *et al.* Crystallin αB acts as a molecular guard in mouse decidualization:
923 Regulation and function during early pregnancy. *FEBS Lett.* **588**, 2944–2951 (2014).
924 79. Niu, W. *et al.* Single-Cell Profiling Uncovers the Roles of Endometrial Fibrosis and
925 Microenvironmental Changes in Adenomyosis. *J. Inflamm. Res.* **Volume 16**, 1949–1965
926 (2023).
927 80. Barra, F. *et al.* Endometriosis Classification and The Role of Tumor Necrosis Factor-Alpha
928 Polymorphisms as A Therapeutic Target. *Int. J. Fertil. Steril.* **14**, (2020).
929 81. Tosti, C., Pinzauti, S., Santulli, P., Chapron, C. & Petraglia, F. Pathogenetic Mechanisms
930 of Deep Infiltrating Endometriosis. *Reprod. Sci.* **22**, 1053–1059 (2015).
931 82. Huang, E., Wang, X. & Chen, L. Regulated Cell Death in Endometriosis. *Biomolecules* **14**,
932 142 (2024).
933 83. Xie, Z.-W., He, Y., Feng, Y.-X. & Wang, X.-H. Identification of programmed cell death-
934 related genes and diagnostic biomarkers in endometriosis using a machine learning and
935 Mendelian randomization approach. *Front. Endocrinol.* **15**, 1372221 (2024).
936 84. Nathan, E. & Tzahor, E. sFRPs: a declaration of (Wnt) independence. *Nat. Cell Biol.* **11**,
937 13–13 (2009).
938 85. Albertsen, H. M. & Ward, K. Genes Linked to Endometriosis by GWAS Are Integral to
939 Cytoskeleton Regulation and Suggests That Mesothelial Barrier Homeostasis Is a Factor in
940 the Pathogenesis of Endometriosis. *Reprod. Sci.* **24**, 803–811 (2017).
941 86. Yang, Y.-M. & Yang, W.-X. Epithelial-to-mesenchymal transition in the development of
942 endometriosis. *Oncotarget* **8**, 41679–41689 (2017).
943 87. Cannito, S. *et al.* Redox mechanisms switch on hypoxia-dependent epithelial–
944 mesenchymal transition in cancer cells. *Carcinogenesis* **29**, 2267–2278 (2008).

945 88. Wu, R.-F. *et al.* High expression of ZEB1 in endometriosis and its role in 17β-estradiol-
946 induced epithelial-mesenchymal transition. *Int. J. Clin. Exp. Pathol.* **11**, 4744–4758 (2018).
947 89. Liu, H. *et al.* Hypoxia-inducible factor-1α promotes endometrial stromal cells migration and
948 invasion by upregulating autophagy in endometriosis. *Reproduction* **153**, 809–820 (2017).
949 90. Konrad, L. *et al.* Similar Characteristics of Endometrial and Endometriotic Epithelial Cells.
950 *Reprod. Sci.* **26**, 49–59 (2019).
951 91. Pally, D. & Naba, A. Extracellular matrix dynamics: A key regulator of cell migration across
952 length-scales and systems. *Curr. Opin. Cell Biol.* **86**, 102309 (2024).
953 92. Shi-Wen, X., Leask, A. & Abraham, D. Regulation and function of connective tissue growth
954 factor/CCN2 in tissue repair, scarring and fibrosis. *Cytokine Growth Factor Rev.* **19**, 133–
955 144 (2008).
956 93. Cook, C. J., Wiggin, N. & Fogg, K. C. Characterizing the Extracellular Matrix Transcriptome
957 of Endometriosis. *Reprod. Sci.* **31**, 413–429 (2024).
958 94. Nanda, A. *et al.* Cytokines, Angiogenesis, and Extracellular Matrix Degradation are
959 Augmented by Oxidative Stress in Endometriosis. *Ann. Lab. Med.* **40**, 390–397 (2020).
960 95. Xiong, W., Zhang, L., Xiong, Y., Liu, H. & Liu, Y. Hypoxia Promotes Invasion of
961 Endometrial Stromal Cells via Hypoxia-Inducible Factor 1α Upregulation-Mediated β-
962 Catenin Activation in Endometriosis. *Reprod. Sci.* **23**, 531–541 (2016).
963 96. Bui, T. M., Wiesolek, H. L. & Sumagin, R. ICAM-1: A master regulator of cellular responses
964 in inflammation, injury resolution, and tumorigenesis. *J. Leukoc. Biol.* **108**, 787–799 (2020).
965 97. Neefjes, J., Jongsma, M. L. M., Paul, P. & Bakke, O. Towards a systems understanding of
966 MHC class I and MHC class II antigen presentation. *Nat. Rev. Immunol.* **11**, 823–836
967 (2011).
968 98. Jiang, L. *et al.* Down-regulation of HLA-DRs and HLA-DPs reflects the deficiency of
969 antigen-presenting cells in endometrium from infertile women with and without ovarian
970 endometriosis. *Hum. Fertil.* **25**, 716–727 (2022).

971 99. Ishii, K. Associations between patients with endometriosis and HLA class II; the analysis of
972 HLA-DQB1 and HLA-DPB1 genotypes. *Hum. Reprod.* **18**, 985–989 (2003).
973 100. Böttcher, J. P. *et al.* NK Cells Stimulate Recruitment of cDC1 into the Tumor
974 Microenvironment Promoting Cancer Immune Control. *Cell* **172**, 1022-1037.e14 (2018).
975 101. Feng, X. *et al.* Analysis of differences in the transcriptomic profiles of eutopic and ectopic
976 endometriums in women with ovarian endometriosis. *PeerJ* **9**, e11045 (2021).
977 102. Islimye Taskin, M. *et al.* Granzyme B levels and granzyme B polymorphisms in peripheral
978 blood of patients with endometriosis: a preliminary study. *J. Obstet. Gynaecol.* **41**, 94–99
979 (2021).
980 103. Burmenskaya, B. O. V. *et al.* Search for personalized implantation window markers in
981 women in an in vitro fertilization program by identifying the transcriptional profile of genes.
982 *Akush. Ginekol. (Sofiia)* **5_2017**, 72–80 (2017).
983 104. Altmäe, S. *et al.* Meta-signature of human endometrial receptivity: a meta-analysis and
984 validation study of transcriptomic biomarkers. *Sci. Rep.* **7**, 10077 (2017).
985 105. Kocbek, V., Vouk, K., Bersinger, N. A., Mueller, M. D. & Lanišnik Rižner, T. Panels of
986 Cytokines and Other Secretory Proteins as Potential Biomarkers of Ovarian Endometriosis.
987 *J. Mol. Diagn.* **17**, 325–334 (2015).
988 106. Kocbek, V., Vouk, K., Mueller, M. D., Rižner, T. L. & Bersinger, N. A. Elevated glycodelin-A
989 concentrations in serum and peritoneal fluid of women with ovarian endometriosis.
990 *Gynecol. Endocrinol.* **29**, 455–459 (2013).
991 107. Meola, J. *et al.* Glycodelin expression in the endometrium of healthy women and in the
992 eutopic and ectopic endometrium of women with endometriosis. *Fertil. Steril.* **91**, 1676–
993 1680 (2009).
994 108. Nisenblat, V. *et al.* Blood biomarkers for the non-invasive diagnosis of endometriosis.
995 *Cochrane Database Syst. Rev.* **2016**, CD012179 (2016).

996 109. Focarelli, R. *et al.* Dysregulation of GdA Expression in Endometrium of Women With
997 Endometriosis: Implication for Endometrial Receptivity. *Reprod. Sci.* **25**, 579–586 (2018).
998 110. Marsh, E. E. *et al.* Burden, Prevalence, and Treatment of Uterine Fibroids: A Survey of
999 U.S. Women. *J. Womens Health 2002* **27**, 1359–1367 (2018).
1000 111. Noyes, R. W., Hertig, A. T. & Rock, J. Dating the endometrial biopsy. *Am. J. Obstet.*
1001 *Gynecol.* **122**, 262–263 (1975).
1002 112. Sheldon, E. *et al.* Biobanking human endometrial tissue and blood specimens: standard
1003 operating procedure and importance to reproductive biology research and diagnostic
1004 development. *Fertil. Steril.* **95**, 2120-2122.e12 (2011).
1005 113. Kang, H. M. *et al.* Multiplexed droplet single-cell RNA-sequencing using natural genetic
1006 variation. *Nat. Biotechnol.* **36**, 89–94 (2018).
1007 114. Kang, M., Ragan, B. G. & Park, J.-H. Issues in Outcomes Research: An Overview of
1008 Randomization Techniques for Clinical Trials. *J. Athl. Train.* **43**, 215–221 (2008).
1009 115. Zheng, G. X. Y. *et al.* Massively parallel digital transcriptional profiling of single cells. *Nat.*
1010 *Commun.* **8**, 14049 (2017).
1011 116. Butler, A., Hoffman, P., Smibert, P., Papalexi, E. & Satija, R. Integrating single-cell
1012 transcriptomic data across different conditions, technologies, and species. *Nat. Biotechnol.*
1013 **36**, 411–420 (2018).
1014 117. Korsunsky, I. *et al.* Fast, sensitive and accurate integration of single-cell data with
1015 Harmony. *Nat. Methods* **16**, 1289–1296 (2019).
1016 118. Wang, W. *et al.* Single-cell transcriptomic atlas of the human endometrium during the
1017 menstrual cycle. *Nat. Med.* **26**, 1644–1653 (2020).
1018 119. Aran, D. *et al.* Reference-based analysis of lung single-cell sequencing reveals a
1019 transitional profibrotic macrophage. *Nat. Immunol.* **20**, 163–172 (2019).

1020 120. Sandberg, T. P. *et al.* Increased expression of cancer-associated fibroblast markers at the
1021 invasive front and its association with tumor-stroma ratio in colorectal cancer. *BMC Cancer*
1022 **19**, 284 (2019).
1023 121. Shi, J.-W. *et al.* An IGF1-expressing endometrial stromal cell population is associated with
1024 human decidualization. *BMC Biol.* **20**, 276 (2022).
1025 122. Queckbörner, S. *et al.* Stromal Heterogeneity in the Human Proliferative Endometrium—A
1026 Single-Cell RNA Sequencing Study. *J. Pers. Med.* **11**, 448 (2021).
1027 123. Yang, Y., Liu, S. & Xiao, X. TOP2A Promotes Proliferation, Migration, and Inflammatory
1028 Response in M5-Treated Keratinocytes by Binding CTBP1 to Activate Wnt/β-Catenin
1029 Signaling. *Cell Biochem. Biophys.* (2024) doi:10.1007/s12013-024-01620-2.
1030 124. Xie, T. *et al.* Single-Cell Deconvolution of Fibroblast Heterogeneity in Mouse Pulmonary
1031 Fibrosis. *Cell Rep.* **22**, 3625–3640 (2018).
1032 125. Wu, B. *et al.* Cell atlas of human uterus. Preprint at https://doi.org/10.1101/267849 (2018).
1033 126. Seccia, T. M. *et al.* Endothelin-1 Drives Epithelial-Mesenchymal Transition in Hypertensive
1034 Nephroangiosclerosis. *J. Am. Heart Assoc.* **5**, e003888 (2016).
1035 127. Lourenço, A. R. & Coffer, P. J. SOX4: Joining the Master Regulators of Epithelial-to-
1036 Mesenchymal Transition? *Trends Cancer* **3**, 571–582 (2017).
1037 128. Castro-Muñozledo, F., Meza-Aguilar, D. G., Domínguez-Castillo, R., Hernández-Zequinely,
1038 V. & Sánchez-Guzmán, E. Vimentin as a Marker of Early Differentiating, Highly Motile
1039 Corneal Epithelial Cells. *J. Cell. Physiol.* **232**, 818–830 (2017).
1040 129. Finak, G. *et al.* MAST: a flexible statistical framework for assessing transcriptional changes
1041 and characterizing heterogeneity in single-cell RNA sequencing data. *Genome Biol.* **16**,
1042 278 (2015).
1043 130. Yu, G., Wang, L.-G., Han, Y. & He, Q.-Y. clusterProfiler: an R Package for Comparing
1044 Biological Themes Among Gene Clusters. *OMICS J. Integr. Biol.* **16**, 284–287 (2012).
1045

Acknowledgements

This work has been supported by NIH NICHD [P50 HD055764]. F.V. discloses support for the research of this work from Carlos III Institute of Health grant [PI21/00528 and PI24/01784], Spanish State Research Agency [CNS2022-135696], Conselleria de Innovacion, Universidad y Ciencia [CIAICO 2022/242], F.V and C.S disclose support from the European Commission Grant Agreement [101080219-2].

We thank INCLIVA Biobank (Hospital Clínico de Valencia) for providing subset of the samples used in this project.

The authors thank all members of the Sirota and Fragiadakis Lab for useful comments and feedback. We also thank Jessica Neely MD, Camilla Wibrand and Emily Teets for helpful advice.

Author Contributions

Conceptualization by A.A, W.W, S.H, U.K, C.P, T.T.O, D.H, J.I, A.C, M.S, G.F, L.G. Data Curation A.A, S.H, W.W. Formal Analysis A.A, W.W, E.T. Funding Acquisition S.H, C.S, F.V, L.G. Sample Collection S.H, C.S, F.V, C.N. Sample Processing S.H, D.K, K.C.V, A.C. Supervision A.C, M.S, G.F, L.G. Validation X.T, E.T. Writing Original Draft, A.A, X.T, B.L. Manuscript Editing and Reviewing: All authors.

Competing interest

The authors declare no competing interests.

1065

1066 # Figure legends

1067 **Figure 1: Data and preprocessing.**

1068 A. Patient cohort and number of samples p srofiled. Classified by disease status and
1069 menstrual cycle phase.

1070 B. Experimental and bioinformatic processing workflow summary.

1071 **Figure 2: Single-cell analysis of endometrial tissue to examine the molecular differences**
1072 **in endometriosis patients across disease states and menstrual cycle phase.**

1073 A. Global UMAP visualization of all sequenced cells, depicting six major broad cell types.

1074 B. UMAP plot colored by the menstrual cycle phase of the samples.

1075 C. UMAP plot displaying samples by disease status: endometriosis, pristine controls, and
1076 fibroid controls.

1077 D. PCA composition colored by menstrual cycle phase.

1078 E. PCA composition colored by disease status.

1079 F. Study design for differential gene expression analysis. Samples were stratified by phase
1080 to compare pristine controls with endometriosis samples. Differential expression was
1081 assessed with $P<0.05$ and log2 fold change (log2 FC) > 0.25. Analyses were performed
1082 using MAST, with p values adjusted.

1083 G. Differentially expressed genes in stratified proliferative samples across major cell types.
1084 Upregulated genes in endometriosis are shown in red (log2 FC > 0.25), while
1085 downregulated genes are shown in blue (log2 FC < -0.25). An UpSet plot illustrates the
1086 overlap of genes exhibiting expression changes across different cell types.

1087 H. Differentially expressed genes in stratified secretory samples across major cell types

1088

1089 **Figure 3: Phase-specific expression in stromal fibroblasts and vascular smooth muscle**
1090 **cells reveals stress, apoptosis, and immune response pathways in endometriosis**
1091 **patients.**

1092 A. UMAP visualization of stromal cell subtypes, color-coded by major tissue type classes
1093 (as shown in Fig. 1A).
1094 B. Log2FoldChange of DEG in the secretory and proliferative phase, comparing pristine
1095 controls and endometriosis samples. Samples were stratified by menstrual phase. DGE
1096 was assessed using a threshold of p-adj.<0.05 and |log2FC| > 0.25.
1097 C. Upregulated pathways in all stromal populations in secretory phase. Showing
1098 Normalized Enrichment Score (NES), p-adj <0.05.
1099 D. UMAP visualization of 8 stromal cell subtypes, color-coded by subtype identity.
1100 E. Top marker genes for each of the 8 stromal cell subtypes.
1101 F. Boxplot showing differential abundance of stromal cell types across samples. Statistical
1102 significance was determined using a t-test and corrected p-values.
1103 G. Number of DEGs comparing control and endometriosis samples for each stromal
1104 subtype, stratified by menstrual phase. Red, upregulated in endometriosis, blue
1105 downregulated in endometriosis.
1106 H. Differentially regulated genes between pristine controls and endometriosis samples,
1107 stratified by menstrual phase. Bolded genes are involved in selected pathways of stress,
1108 apoptosis, and immune signaling.
1109 I. Pathway analysis of upregulated biological processes in stromal subpopulations,
1110 stratified by proliferative and secretory. Showing Normalized Enrichment Score (NES),
1111 p-adj <0.05 with selected pathways highlighted in bold.

1112 **Figure 4: Epithelial subpopulations show upregulation of epithelium migration in**
1113 **endometriosis patients.**

1114 A. UMAP visualization of epithelial cell subtypes, color-coded by major tissue populations
1115 (as shown in Fig. 1A).
1116 B. Log2FoldChange of DEG in the secretory and proliferative phase unciliated epithelia,
1117 comparing pristine controls and endometriosis samples. Samples were stratified by
1118 menstrual phase. DGE was assessed using a threshold of p-adj.<0.05 and |log2FC| >
1119 0.25.
1120 C. Upregulated pathways in all unciliated epithelial populations in the secretory phase.
1121 Showing Normalized Enrichment Score (NES), p-adj <0.05.
1122 D. UMAP visualization of epithelial cell subtypes, color-coded by specific tissue type
1123 classes.
1124 E. Top marker genes for epithelial subtype.
1125 F. Number of DEGs comparing control and endometriosis samples per epithelial population
1126 stratified by menstrual phase. Red, upregulated in endometriosis, blue downregulated in
1127 endometriosis
1128 G. Differentially regulated genes between pristine controls and endometriosis samples,
1129 stratified by menstrual phase. Bolded genes are involved in selected pathways of cell
1130 death, locomotion, migration and adhesion.
1131 H. Pathway analysis of upregulated biological processes in epithelial subpopulations.
1132 Showing Normalized Enrichment Score (NES), p-adj <0.05 with selected pathways
1133 highlighted in bold.
1134 **Figure 5: Uterine NK cells demonstrate augmented activity during endometriosis.**
1135 A. UMAP overview depicting fine-grained immune subtypes.
1136 B. Selected marker genes for each subpopulation.
1137 C. Number of DEGs comparing pristine control and endometriosis samples per immune
1138 population, stratified by menstrual phase. Red, upregulated in endometriosis, blue
1139 downregulated in endometriosis.

1140 D. Differentially regulated genes in macrophages, NK cells, and CD8+ T-cells, between
1141 pristine controls and endometriosis samples, stratified by menstrual phase.
1142 E. Pathway analysis of upregulated biological processes in NK cells. Showing Normalized
1143 Enrichment Score (NES), p-adj <0.05.

1144 **Figure 6: In-silico prediction shows upregulated communication in extracellular matrix**
1145 **and inflammatory pathways in disease**

1146 A. Summary of differential predicted pathways stratified by phase, color by log2-fold
1147 change and stratified by menstrual phase.
1148 B. Pathway differences in the proliferative phase. P-value < 0.05, top 10% of interactions.
1149 Red represents increase in endometriosis compared to pristine controls; blue represents
1150 decrease.
1151 C. Probability of communication with Innate lymphoid cells as the source in the proliferative
1152 phase, colored by Log2FC differences between endometriosis and controls.
1153 D. Pathway differences in the secretory phase. P-value <05, top 10% of interactions. Red
1154 represents increase in endometriosis compared to pristine controls; blue represents
1155 decrease.
1156 E. Probability of communication with VSM cells as the source in the secretory phase,
1157 colored by Log2FC differences between endometriosis and pristine controls.

Figure 1. Data and preprocessing

A.

	Proliferative phase (n)	Secretory phase (n)	Total (n)
Endometriosis I - II	5	8	25
Endometriosis III - IV	5	7	
Fibroid controls	4	6	10
Pristine controls	5	3	8
Total (n)	19	24	43

B.

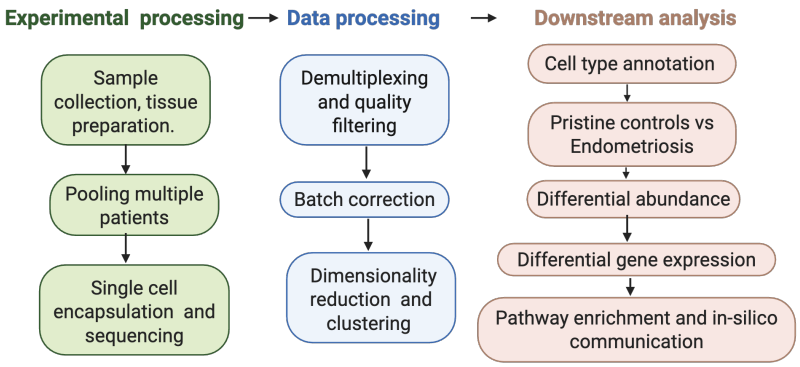

Figure 2. Single-cell analysis of endometrial tissue to examine the molecular differences in endometriosis patients across disease states and menstrual cycle phase.

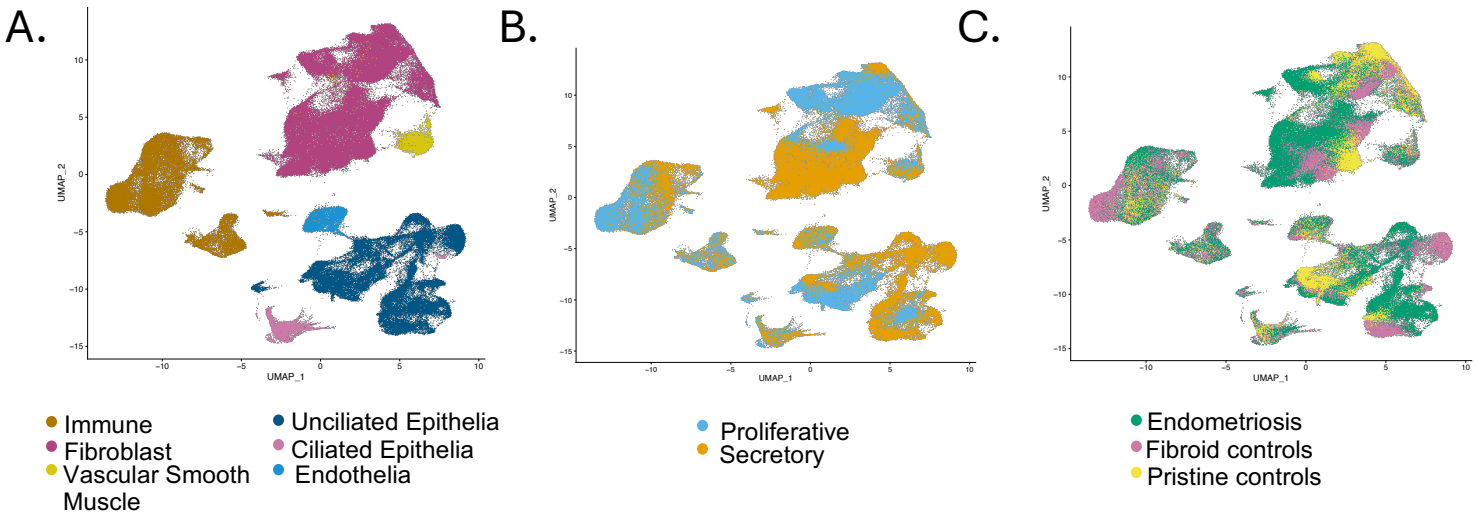

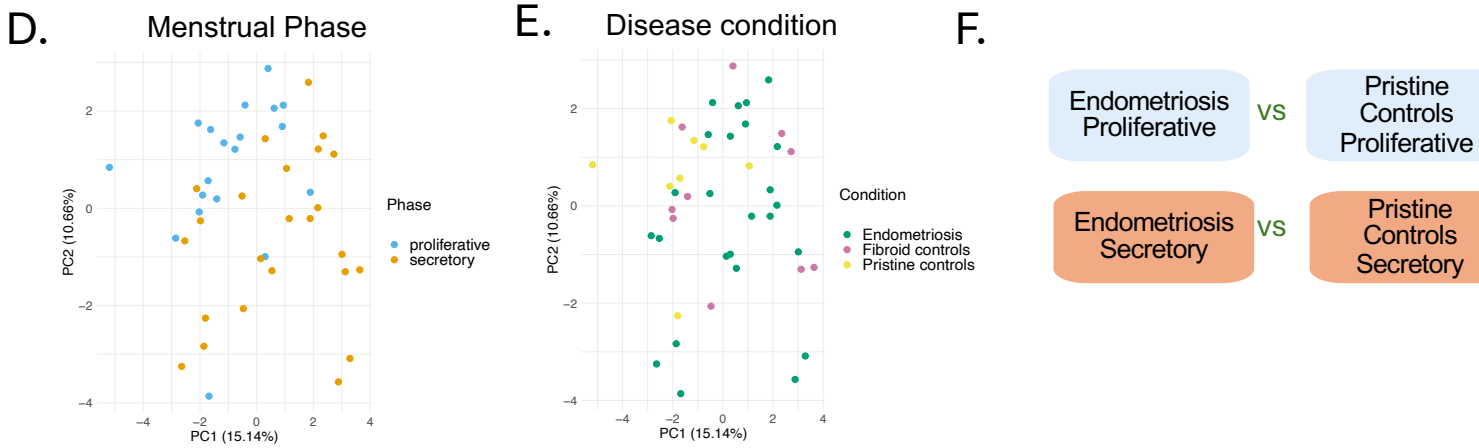

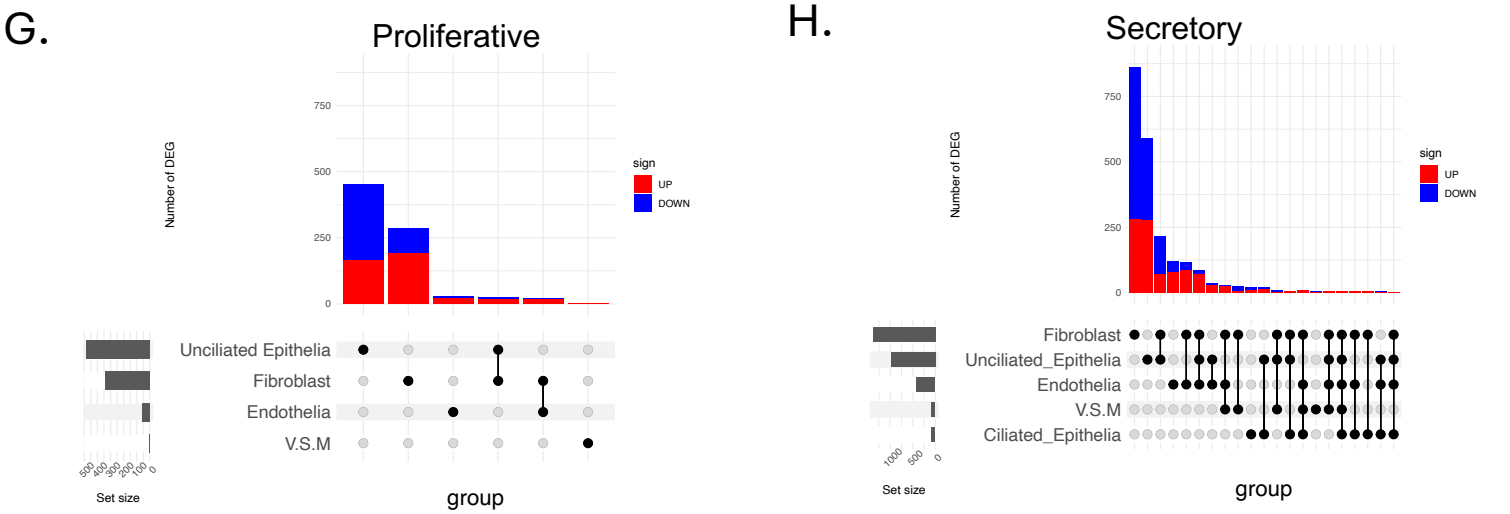

Figure 3. Phase-specific expression in stromal fibroblasts and vascular smooth muscle cells reveals stress, apoptosis, and immune response pathways in endometriosis patients.

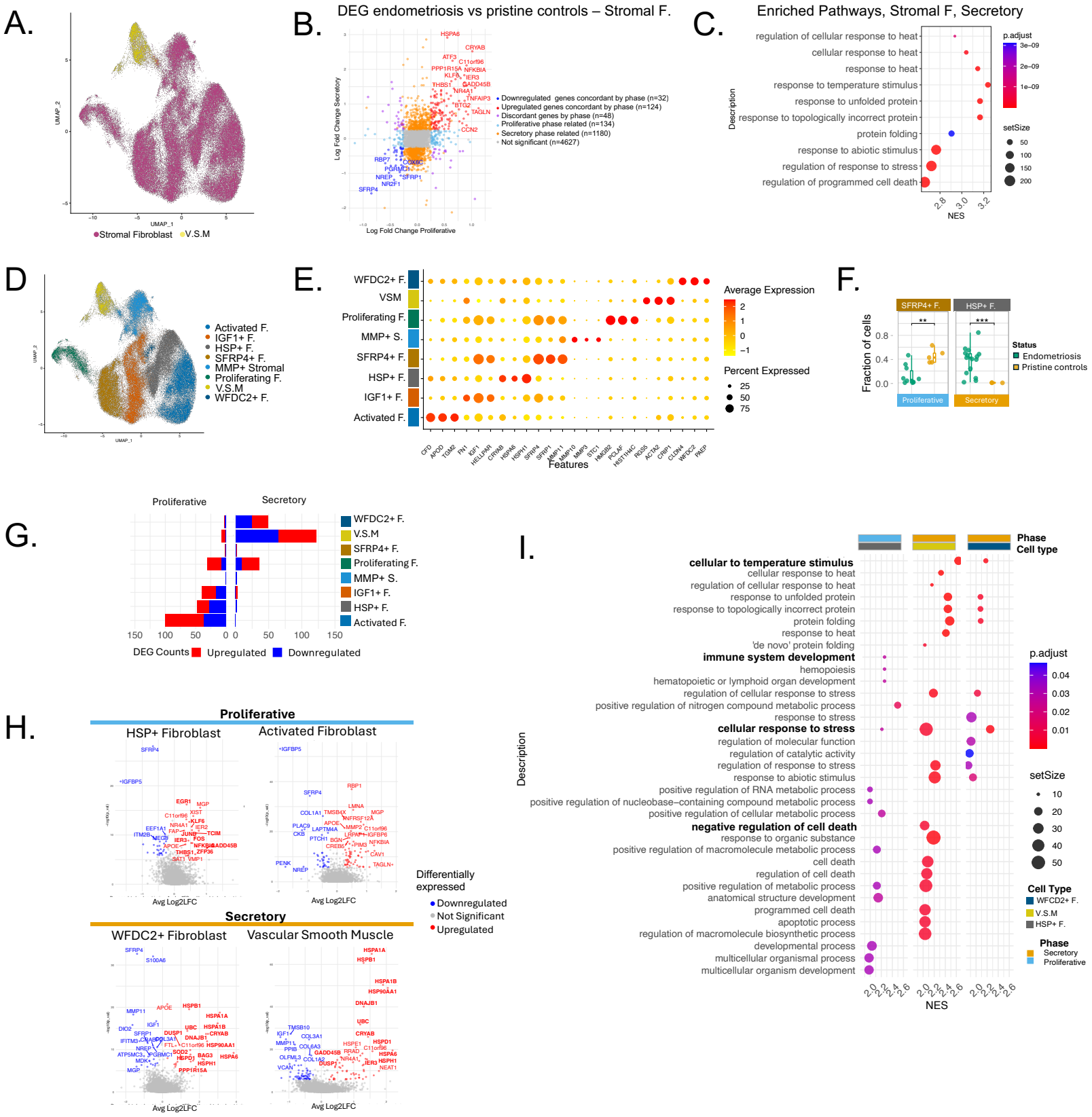

Figure 4. Epithelial subpopulations show upregulation of epithelium migration in endometriosis patients.

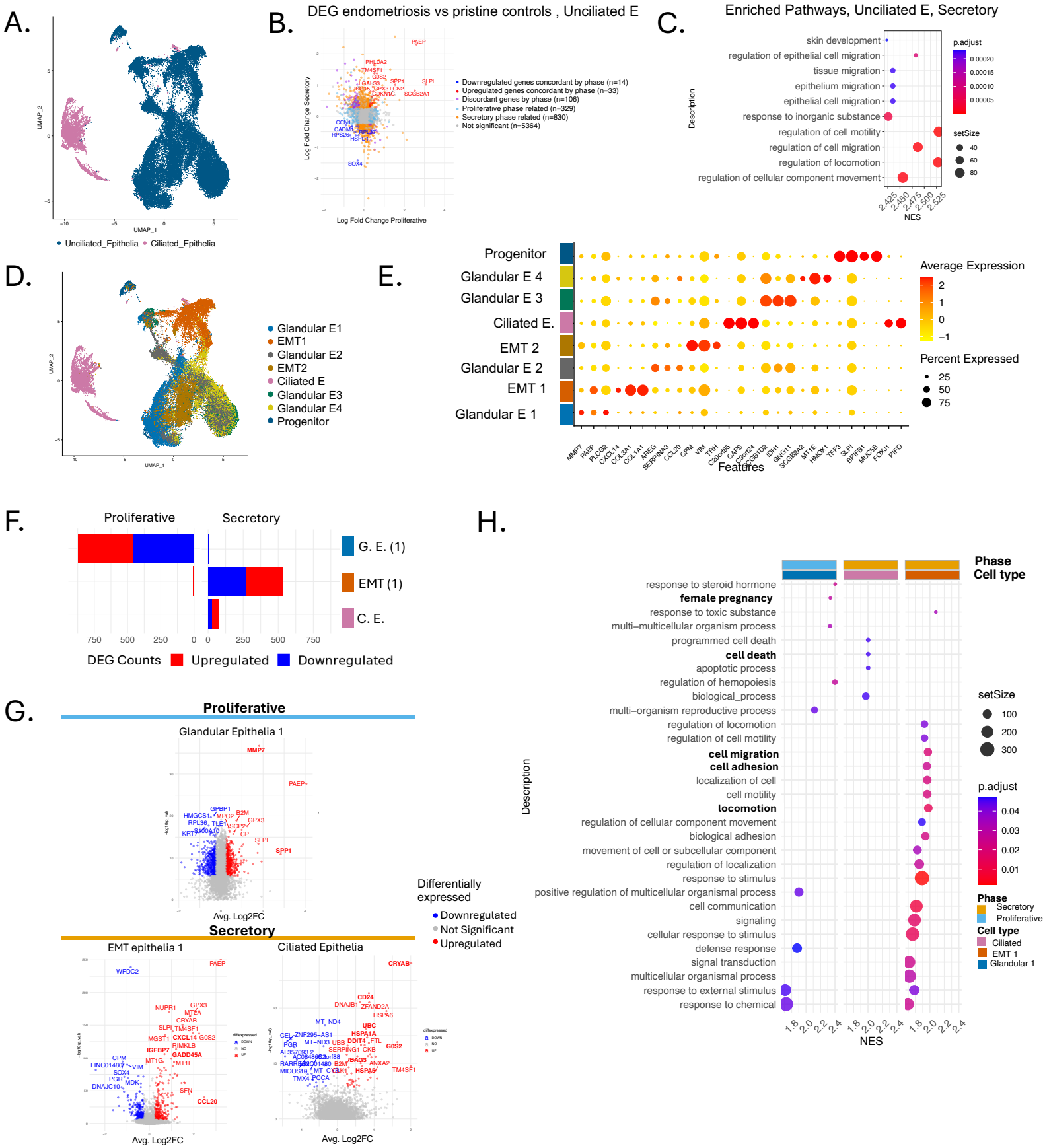

Figure 5. Uterine NK cells demonstrate augmented activity during endometriosis.

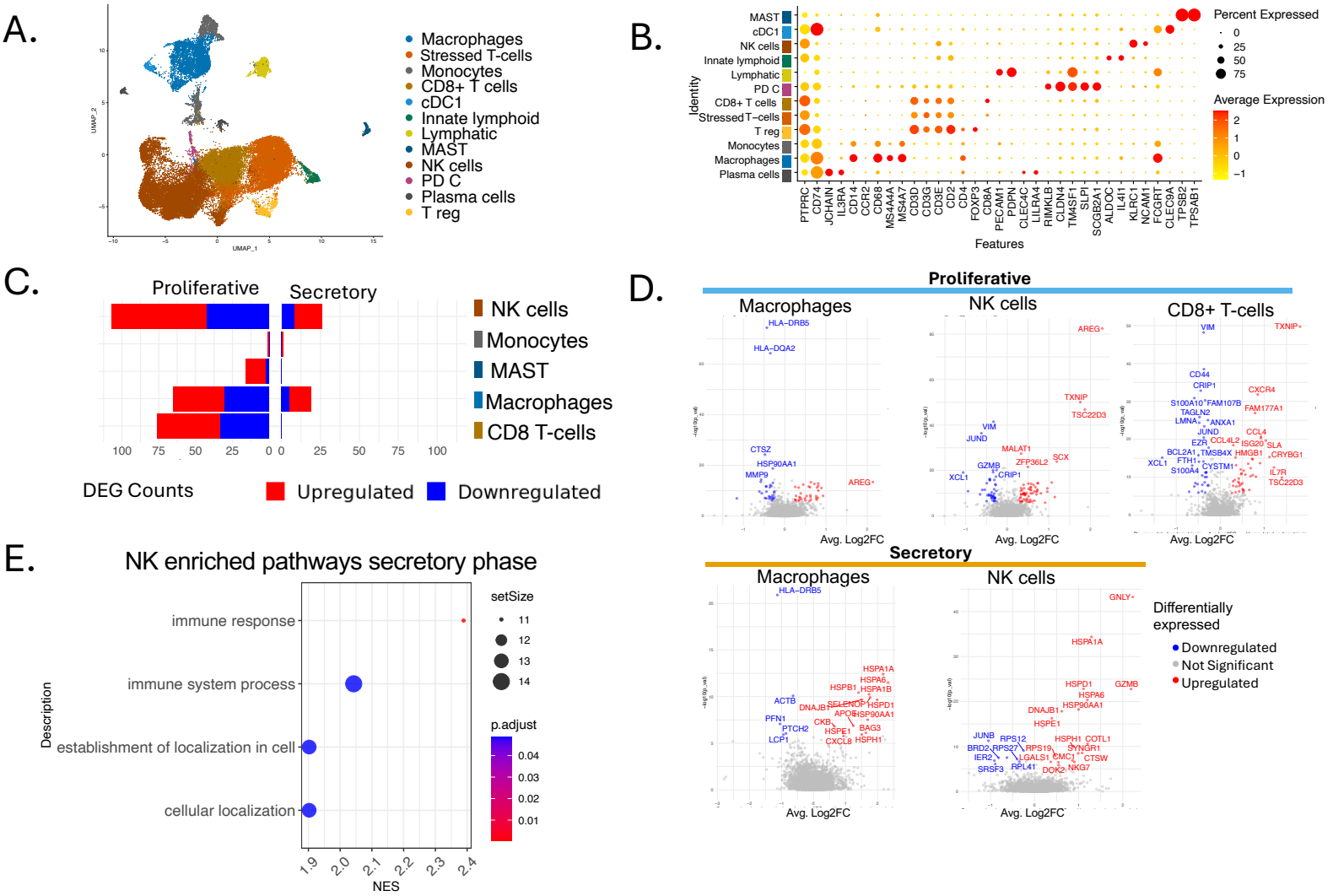
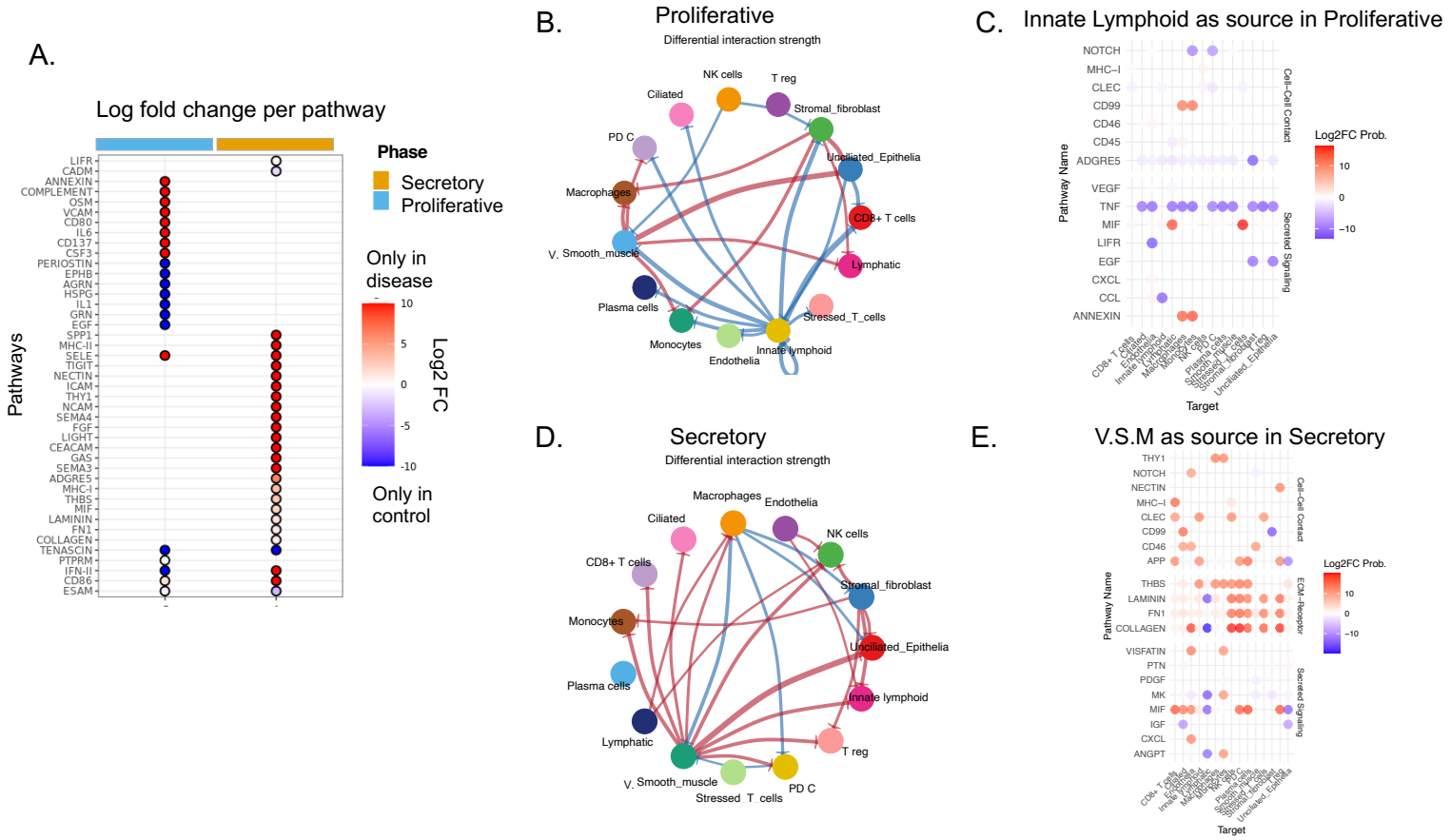
Figure 6. In-silico prediction shows upregulated communication in extracellular matrix and inflammatory pathways in disease.